Trans. Phenom. Nano Micro Scales, 8(1): 39-60, Winter and Spring 2020
DOI: 10.22111/tpnms.2019.25210.1154

ORIGINAL RESEARCH PAPER

Free Vibration Analysis of SVC Systems Based on Reddy-Levinson Model Using DQM

Hadi Mohammadi Hooyeh[1,*] , Ali Mohammadi Hooyeh[2] , Hasan Afshari[3]

[1]*Department of Solid Mechanics, Faculty of mechanical Engineering, University of Eyvanekey, Garmsar/Semnan, Iran*
[2]*Department of Solid Mechanics, Faculty of mechanical Engineering, Sharif University of Technology, Tehran, Iran*
[3]*Department of Mechanical Engineering, Khomeinishahr Branch, Islamic Azad University, Khomeinishahr/Isfahan, Iran*

Received 18 May 2018; revised 9 November 2019; accepted 10 November 2019; available online 22 February 2020

ABSTRACT: In this study, the free vibration analysis of smart vibration control (SVC) systems based on Reddy – Levinson model and modified strain gradient theory is developed. This system consist of a micro beam at middle and two magneto-electro-elastic (MEE) composite micro beams at top and bottom which connected by enclosing elastic medium and simulated by Winkler and Pasternak foundation. The effects of the lower MEE composite micro beam in the absence of upper MEE composite micro beam and also the effect of both MEE composite micro beams together on the dimensionless natural frequency of the middle micro beam are evaluated. It is shown that the presence of both MEE composite micro beams together have less dimensionless natural frequency than presence of lower MEE composite micro beam alone. The results of this work can be useful to analysis, design and manufacture intelligent micro-systems to hamper resonance phenomenon or as a sensor to control the dynamic stability of micro structures.

KEYWORDS*: Free Vibration analysis; Reddy - Levinson model; Smart vibration control system; three micro- and micro-composite beams*

INTRODUCTION

Smart vibration control systems (SVCS) due to its unique properties have attracted the attention of many the research communities. The SVCS has been widely extended in micro- and nano-scale devices and systems such as thin films atomic force microscopes (AFMS) [1-3], micro- and nanoelectro-mechanical systems (MEMS) and NEMS)[4]. Magneto electro elastic (MEE) micro and nanocomposite materials are the main components of SVCS [5-7]. MEE materials have the unique ability of converting the system energy from one form to the other (among magnetic, electric and mechanical energies) [8-9]. A literature review represents that the mechanical behavior of SVCS and MEE structural elements have been investigated by several researchers. Nonlinear vibration of a nanobeam (NB) coupled with a piezoelectric nanobeam (PNB) based on the strain gradient theory in conjunction with the Euler-Bernoulli beam model is investigated by Ghorbanpour Arani et al. [10] They considered that the PNB is subjected to an external electric voltage in thickness direction and a uniform temperature change. Their results indicated that the dimensionless frequency of NB reduces because of increasing the external electric voltage. Pisarskia et al. [11] Buckling behavior of nonlocal MEE functionally graded (FG) beams based on a higher-order beam model is represented by Ebrahimi and Barati [12]. It is obvious from their results that the magnetic and electric fields, nonlocal parameter, power-law index parameter, power-law index and slenderness ratio parameter, power-law index and slenderness ratio have significant effects on the buckling behavior of MEE-FG nanobeams. Vaezi et al. [13] obtained natural frequencies and buckling loads of a MEE simply supported microbeam under electric and magnetic potentials.

Their results revealed that by increasing of the value of length-to-thickness ratio is higher than the values of the normalized natural frequency. Nonlocal nonlinear plate model for large amplitude vibration of MEE nanoplates was presented by Farajpour et al. [14].

Kattimani and Ray [15] analyzed active damping of geometrically nonlinear vibrations of MEE-FG plates integrated with the patches of the active constrained layer damping (ACLD) treatment. They proposed the constrained viscoelastic layer of the ACLD treatment is modeled by using a Golla–Hughes–McTavish (GHM) method in time domain. Gharib et al. [16] developed the linear vibrations of a smart thin micro panel of polymeric nano-composite reinforced by the single-walled boron nitride nano-tubes (SWBNNTs) and the matrix Poly-VinyliDene Fluoride (PVDF) on an elastic substrate. Ghorbanpour Arani and his research group [17] addressed wave propagation in embedded nanocomposite polymeric piezoelectric micro plates reinforced by single-walled carbon nanotubes (SWCNTs) using viscoelastic quasi-3D sinusoidal shear deformation theory. Using Eringen's nonlocal theory and analytical solution the dimensionless phase velocity, cut-off and escape frequencies are obtained.

*Corresponding Author Email: *hmohammadihooyeh@eyc.ac.ir*
Tel.: +982177105105; Note. This manuscript was submitted on May 18, 2018; approved on November 10, 2019; published online February 22, 2020.

Nomenclature

A_{ij}^{p}	Weighting coefficients of the pth order derivative	η	Symmetric rotation gradient tensor
b	Thickness of microbeams	θ	Electric potentials
$\bar{d}_{ij}$	Magnetoelectric constant	l	Independent material length scale
E	Electric field	l^{*}	Independent material length scale
E	Young's modulus	m_{ij}	Higher – order stresses
F	Elastic medium	κ	Infinitesimal rotation vector
h	Width of microbeams	$\bar{\lambda}_{i}$	Pyromagnetic constant
H	Magnetic field	μ	Shear modulus
K	Kinetic energy	μ^{*}	Shear modulus
K_{g}	Pasternak's shear modulus	$\bar{v}_{i}$	Pyroelectric constant
K_{w}	Winkler's spring modulus	ρ	Density of MEE composite micro beam
L	Length of microbeams	ρ^{*}	Density of micro beam
N	Grid point's number along x direction	σ_{ij}	Stress tensor
$\{q\}$	Dynamic displacement vector	σ_{ij}^{*}	Classical stress tensor
U	Strain energy	$\tau_{ijk}^{(1)}$	Higher – order stresses
$\bar{u}_{k}$	Displacement vector	φ	Angle of the rotation
V_{E}	External electric	χ	Symmetric rotation gradient tensor
w	Z component of the displacement vector	ϕ_{E}	Variation of electric
x, y , z	Components of thedisplacement	ω	Dimensionless natural frequency
	Greek Symbols	Υ_{H}	Magnetic potentials
$\bar{\alpha}_{ij}$	Magnetic constant	$\hat{\Theta}_{i}$	Components of vibration mode
$\bar{\beta}_{ij}$	Thermal moduli	p_{i}	Higher – order stresses
$\bar{c}_{ij}$	Elastic constant	$\bar{q}_{ij}$	Piezomagnetic constant
$\bar{e}_{ij}$	Piezoelectric constant	$\bar{s}_{ij}$	Dielectric constant
γ	Dilatation gradient tensor	Ω_{H}	External magnetic
Γ	Magnetic potentials	ΔT	Temperature change
δ	Knocker symbol		**Subscripts**
∇^{2}	Laplace vector	i	Number of beams (0,1,2)
ε	Strain tensor	j	Number of MEE

NUMERICAL METHOD

The results of their research illustrated that the cut-off and escape frequencies were decreased with increasing of the small scale parameter. Wang et al. [18] presented vibration analysis of piezoelectric ceramic circular nanoplates considering surface and nonlocal effects. Three-dimensional free vibration of multi layered MEE plates under combined clamped/free lateral boundary conditions using a semi-analytical discrete layer approach was analyzed by Chen et al [19]. Their results showed that considering the magnetostrictive layers as the outer layers in the sandwich MEE laminate yields an increase of an average 6–8% in frequency as compared to the laminate with the piezoelectric layers on the outside. Arefi [20] presented the wave propagation analysis of a functionally graded nano-rod made of MEE material subjected to an electric and magnetic potential. Using Hamilton's principle and nonlocal elasticity theory, the equation of motion is obtained. It is found from his results that the applied voltage and magnetic field have a significant effect in changing the imaginary part of the phase velocity of the nano-rod. Furthermore, the imaginary part of the phase velocity for different values of applied magnetic field and voltage indicates that increasing the applied voltage and magnetic field decreases considerably the dimensionless imaginary part of the phase velocity. Linear and nonlinear free vibration of a multilayered MEE doubly-curved shell resting on an elastic foundation was studied by Shooshtari and Razavi [21]. They employed the Donnell shell theory for achieved equation of motion and Gauss' laws for electrostatics and magnetostatics modeled the electric and magnetic behavior. Their results showed that electric and magnetic potentials have more effect on the nonlinear frequency ratios of MEE shells with smaller thicknesses and radii of curvature. Also, they [22] introduced nonlinear free vibration of symmetric MEE laminated rectangular plates.They showed that using MEE layers in composite plates decreases nonlinear frequency ratio. Also, length-to-thickness ratio has negligible effect on the nonlinear frequency ratio while comparing with the effects of aspect ratio.

Li and Feng [23] proposed the static bending and the free vibration of a simply supported piezoelectric beam based on the modified strain gradient theory and Timoshenko beam theory. Their results depicted that the difference between the natural frequencies predicted by the modified strain gradient model and the classical model are large when the length-thickness ratio of the beam is small.

Also for the static bending, the electric potential, stress and electric displacement that predicted by the modified strain gradient model are smaller than those predicted by the classical Timoshenko beam model. The free vibration of MEE nanobeams based on the nonlocal theory and Timoshenko beam theory is carried out by Ke and Wang [24].

They used the differential quadrature method (DQM) to obtain the natural frequencies and mode shapes of MEE nanobeams.

Their studies revealed that the natural frequency of nonlocal nanobeam is always smaller than that of the classical nanobeam, and it decreases with an increase in the nonlocal parameter.

Ansari et al. [25] examined a nonlocal geometrically nonlinear beam model for MEE nanobeams subjected to external electric voltage, external magnetic potential and uniform temperature rise. In the other work, Ansari et al. [26] developed the forced vibration behavior of nonlocal third-order shear deformable beam model of magneto - electro - thermo elastic (METE) nanobeams based on the nonlocal elasticity theory in conjunction with the von Karman geometric nonlinearity. They depicted that increasing either the nonlocal parameter or the slenderness ratio leads to decreasing the natural frequency of nanobeams. Atabakhshian et al. [27] introduced nonlinear electro-thermal vibration and stability of a smart coupled nanobeam system with an internal flow based on nonlocal elasticity theory.

It is concluded from their results that applying an electric voltage on piezoelectric polymeric beam will increase the stability of fluid-conveying nanotube. Mohammadimehr et al. [28] established the buckling and deflection of the double-coupled piezoelectric polymeric nanocomposite rectangular plates reinforced by SWCNTs and SWBNNTs based on modified strain gradient theory embedded in elastic foundation.

Their research revealed that the elastic foundation and van der Waals interaction in contrast to applied voltage increase the dimensionless critical biaxial buckling load and vice versa decrease the dimensionless deflection of the double coupled nanocomposite plates. Also, they [29] exhibited free vibration of viscoelastic double-bonded polymeric nanocomposite plate reinforced by SWCNTs embedded in viscoelastic foundation based on modified strain gradient theory. They found that the non-dimensional natural frequency in out of phase mode is greater than that of in- phase mode.

It is also found that the double bonded nanocomposite plate oscillated as single nanaocomposite plate of in-phase mode.

GEOMETRY OF SYSTEM

The geometry of smart micro- beam system illustrated in Figure 1 that showed the three parallel micro beams. At the middle system, a micro beam is considered that don't have a piezoelectric and magnetostrictive effect. Two MEE composite micro beams embedded at top and bottom of micro beam are considered that the external magnetic potential, external electric potential and temperature change are exposed to them.

It should be noted that the bottom MEE composite microbeam, the middle microbeam and the top MEE composite micro beam are mentioned by 0, 1 and 2 numbers, respectively. The each MEE composite micro beam is connected to the micro beam by elastic foundation.

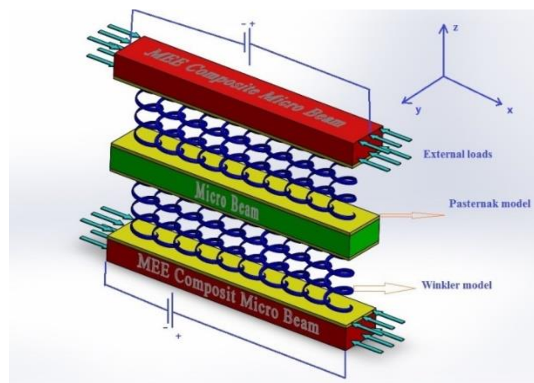

Fig. 1. Schematic figure of the smart micro-beam system

The governing equation of motion for smart micro-beam system

Reddy –Levinson displacement model and kinetic energies

On the basis of the third-order shear deformation beam theory, the displacements field of Reddy-Levinson (R-L) beam can be written as follows [30-32]:

$$\bar{u}_{1i}\left(x,z,t\right)=-z\,\varphi_i\left(x,t\right)-c_1 z^3\left(-\varphi_i\left(x,t\right)+\frac{\partial w_i\left(x,t\right)}{\partial x}\right) \tag{1}$$

$$\bar{u}_{2i}\left(x,z,t\right)=0 \tag{2}$$

$$\bar{u}_{3i}\left(x,z,t\right)=w_i\left(x,t\right) \tag{3}$$

Using equation (1–3) the kinetic energy for each micro beam is given by:

$$K_i=\frac{1}{2}\rho\int_0^L\int_A\left\{\left(\left(\frac{\partial(-z\,\varphi_i(x,t)-c_1z^3(-\varphi_i(x,t)+\frac{\partial w_i(x,t)}{\partial x}))}{\partial t}\right)^2+\left(\frac{\partial w_i}{\partial t}\right)^2\right)\right\}dAdx$$

$$\begin{Bmatrix}K_{0,2}\\K_1\end{Bmatrix}=\frac{1}{2}\int_0^L\left\{\begin{matrix}-c_1^2\begin{Bmatrix}m_6\\m_6^*\end{Bmatrix}(\frac{\partial\varphi_i}{\partial t})^2-2c_1^2\begin{Bmatrix}m_6\\m_6^*\end{Bmatrix}(\frac{\partial\varphi_i}{\partial t})(\frac{\partial^2 w_i}{\partial x\,\partial t})\\+c_1^2\begin{Bmatrix}m_6\\m_6^*\end{Bmatrix}(\frac{\partial^2 w_i}{\partial x\,\partial t})^2\\-2c_1\begin{Bmatrix}m_4\\m_4^*\end{Bmatrix}(\frac{\partial\varphi_i}{\partial t})^2+2c_1\begin{Bmatrix}m_4\\m_4^*\end{Bmatrix}(\frac{\partial\varphi_i}{\partial t})(\frac{\partial^2 w_i}{\partial x\,\partial t})\\+\begin{Bmatrix}m_2\\m_2^*\end{Bmatrix}(\frac{\partial\varphi_i}{\partial t})^2+\begin{Bmatrix}m_0\\m_0^*\end{Bmatrix}(\frac{\partial w_i}{\partial t})^2\end{matrix}\right\}dx \quad (4)$$

where superscript (*) stands for the micro beam (1). Also $\begin{Bmatrix}m_r\\m_r^*\end{Bmatrix}(r=0,2,4,6)$ expressed as:

$$\begin{Bmatrix}m_r\\m_r^*\end{Bmatrix}=\begin{Bmatrix}\rho\\\rho^*\end{Bmatrix}\int_A(1,z^2,z^4,z^6)dA\quad(r=0,2,4,6) \quad (5)$$

The strain energies using modified strain gradient theory

The modified strain gradient elasticity theory that exhibited by Lam[33]and Yang [34] states that the stored strain energy in a continuum constructed by linear MEE composite micro beam and micro beam occupying region, with infinitesimal deformations is given by [35- 37]:

$$\begin{Bmatrix}U_{0,2}\\U_1\end{Bmatrix}=\frac{1}{2}\int_\Omega\left(\begin{matrix}\begin{Bmatrix}\sigma_{ij}\\\sigma_{ij}^*\end{Bmatrix}\varepsilon_{ij}+\begin{Bmatrix}p_i\\p_i^*\end{Bmatrix}\gamma_i+\begin{Bmatrix}\tau_{ijk}^{(1)}\\\tau_{ijk}^{*(1)}\end{Bmatrix}\eta_{ijk}^{(1)}\\+\begin{Bmatrix}m_{ij}\\m_{ij}^*\end{Bmatrix}\chi_{ij}-\begin{Bmatrix}\mathrm{D}_i\mathrm{E}_i+B_iH_i\\0\end{Bmatrix}\end{matrix}\right)dV \quad (6)$$

In which the components of the strain tensor, the dilatation gradient tensor, the deviatoric stretch gradient tensor, the symmetric rotation gradient tensor, the electric field and the magnetic field are respectively denoted by $\varepsilon_{ij},\gamma_i,\eta_{ijk}^{(1)},\chi_{ij},\mathrm{E}_i,H_i$ which are defined as [38-42]:

$$\varepsilon_{ij}=\frac{1}{2}(u_{i,j}+u_{j,i}) \quad (7)$$

$$\gamma_i=\varepsilon_{mm,i} \quad (8)$$

$$\eta_{ijk}^{(1)}=\frac{1}{3}(\varepsilon_{jk,i}+\varepsilon_{ki,j}+\varepsilon_{ij,k})-\frac{1}{15}\delta_{ij}\left(\varepsilon_{mm,k}+2\varepsilon_{mk,m}\right)-\frac{1}{15}\delta_{jk}\left(\varepsilon_{mm,i}+2\varepsilon_{mi,m}\right)-\frac{1}{15}\delta_{ki}\left(\varepsilon_{mm,j}+2\varepsilon_{mj,m}\right) \quad (9)$$

$$\chi_{ij}=\frac{1}{2}(\kappa_{i,j}+\kappa_{j,i})\quad \kappa_i=\frac{1}{2}(\mathrm{curl(u)})_i \quad (10)$$

$$E_i=-\theta_{,i} \quad (11)$$

$$H_i=-\Gamma_{,i} \quad (12)$$

where $u_i,\varepsilon_{mm},\kappa$ and δ_{ij} are the displacement vector, the dilatation strain, the infinitesimal rotation vector and the Knocker symbol respectively. $\{p_i,p_i^*\},\{\tau_{ijk}^{(1)},\tau_{ijk}^{*(1)}\},\{m_{ij},m_{ij}^*\}$, θ and Γ represented the higher – order stresses, the electric represented the higher – order stresses, the electric and the magnetic potentials respectively which may be expressed as follows[41],[43]: and the magnetic potentials respectively which may be expressed as follows[41],[43]:

$$\begin{Bmatrix}p_i\\p_i^*\end{Bmatrix}=2\begin{Bmatrix}\mu l_0^2\\\mu^*l_0^{*2}\end{Bmatrix}\gamma_i \quad (13)$$

$$\begin{Bmatrix}\tau_{ijk}^{(1)}\\\tau_{ijk}^{*(1)}\end{Bmatrix}=2\begin{Bmatrix}\mu l_1^2\\\mu^*l_1^{*2}\end{Bmatrix}\eta_{ijk}^{(1)} \quad (14)$$

$$\begin{Bmatrix}m_{ij}\\m_{ij}^*\end{Bmatrix}=2\begin{Bmatrix}\mu l_2^2\\\mu^*l_2^{*2}\end{Bmatrix}\chi_{ij} \quad (15)$$

$$\theta(\mathrm{x,z,t})=-\cos(\beta\,\mathrm{z})\phi_E(\mathrm{x,t})+\frac{2zV_E}{h},\quad \beta=\frac{\pi}{h} \quad (16)$$

$$\Gamma(\mathrm{x,z,t})=-\cos(\beta\,\mathrm{z})\Upsilon_H(\mathrm{x,t})+\frac{2z\,\Omega_H}{h},\quad \beta=\frac{\pi}{h} \quad (17)$$

MEE Reddy-Levinson (R-L) micro composite beam which is under the plane stress condition, can be written as follows:

$$\begin{bmatrix}\sigma_{xx}\\\sigma_{xz}\\D_x\\D_z\\B_x\\B_z\end{bmatrix}=\begin{bmatrix}\bar{c}_{11}&0&-\bar{e}_{31}&0&-\bar{q}_{31}&0\\0&\bar{c}_{44}&0&-\bar{e}_{15}&0&-\bar{q}_{15}\\0&\bar{e}_{15}&0&\bar{s}_{11}&0&\bar{d}_{11}\\\bar{e}_{31}&0&\bar{s}_{33}&0&\bar{d}_{33}&0\\0&\bar{q}_{15}&0&\bar{d}_{11}&0&\bar{\alpha}_{15}\\\bar{q}_{31}&0&\bar{d}_{33}&0&\bar{\alpha}_{33}&0\end{bmatrix}\begin{bmatrix}\varepsilon_{xx}\\\gamma_{xz}\\E_z\\E_x\\H_z\\H_x\end{bmatrix}+\begin{bmatrix}-\bar{\beta}_1\\0\\0\\\bar{\nu}_3\\0\\\bar{\lambda}_3\end{bmatrix}\Delta T \quad (18)$$

$\bar{c}_{ij},\bar{e}_{ij},\bar{q}_{ij},\bar{s}_{ij},\bar{\beta}_{ij},\bar{d}_{ij},\bar{\alpha}_{ij},\bar{\nu}_i$ and $\bar{\lambda}_i$ are constants that given at Appendix (A-1).

The classical stress tensor σ_{ij}^* for micro – beam can be obtained as follows:

$$\sigma_{ij}^*=\lambda^*\delta_{ij}\varepsilon_{kk}+2\mu^*\varepsilon_{ij} \quad (19)$$

where [46]:

$$\lambda^*=\frac{E\nu}{(1+\nu)(1-2\nu)}\qquad \mu^*=\frac{E}{2(1+\nu)} \quad (20)$$

By substituting equations (1-3) into equation 7, the components of normal and shear strains for R-L beam model are obtained as:

$$\varepsilon_{xx} = -z\,\frac{\partial \varphi}{\partial x} - c_1 z^3\left(-\frac{\partial \varphi}{\partial x} + \frac{\partial^2 w}{\partial x^2}\right) \tag{21}$$

$$\varepsilon_{xz} = \frac{1}{2}\left(\frac{\partial w}{\partial x} - \varphi - 3c_1 z^2\left(-\varphi + \frac{\partial w}{\partial x}\right)\right) \tag{22}$$

By employing equation 8, 21 and 22, the non-zero components of dilatation gradient tensor are as the following form:

$$\gamma_x = -z\,\frac{\partial^2 \varphi}{\partial x^2} - c_1 z^3\left(-\frac{\partial^2 \varphi}{\partial x^2} + \frac{\partial^3 w}{\partial x^3}\right) \tag{23}$$

$$\gamma_z = -\frac{\partial \varphi}{\partial x} - 3c_1 z^2\left(-\frac{\partial \varphi}{\partial x} + \frac{\partial^2 w}{\partial x^2}\right) \tag{24}$$

Using equations 9, 21 and 22, the non-zero component of deviatoric stretch gradient tensor are obtained as:

$$\begin{aligned}
&\eta_{111}^{(1)} = -\frac{2}{5} z \frac{\partial^2 \varphi}{\partial x^2} - \frac{2}{5} c_1 z^3\left(-\frac{\partial^2 \varphi}{\partial x^2} + \frac{\partial^3 w}{\partial x^3}\right) \\
&+\frac{6}{5} c_1 z\left(-\varphi + \frac{\partial w}{\partial x}\right) \\
&\eta_{333}^{(1)} = \frac{2}{5}\frac{\partial \varphi}{\partial x} - \frac{1}{5}\frac{\partial^2 w}{\partial x^2} + \frac{6}{5} c_1 z^2\left(-\frac{\partial \varphi}{\partial x} + \frac{\partial^2 w}{\partial x^2}\right) \\
&\eta_{113}^{(1)} = \eta_{131}^{(1)} = \eta_{311}^{(1)} = -\frac{8}{15}\frac{\partial \varphi}{\partial x} + \frac{4}{15}\frac{\partial^2 w}{\partial x^2} \\
&-\frac{8}{5} c_1 z^2\left(-\frac{\partial \varphi}{\partial x} + \frac{\partial^2 w}{\partial x^2}\right) \\
&\eta_{313}^{(1)} = \eta_{331}^{(1)} = \eta_{133}^{(1)} = -\frac{8}{5} c_1 z\left(-\varphi + \frac{\partial w}{\partial x}\right) + \frac{z}{5}\frac{\partial^2 \varphi}{\partial x^2} \\
&+\frac{z^3}{5} c_1\left(-\frac{\partial^2 \varphi}{\partial x^2} + \frac{\partial^3 w}{\partial x^3}\right) \\
&\eta_{122}^{(1)} = \eta_{212}^{(1)} = \eta_{221}^{(1)} = \frac{2}{5} c_1 z\left(-\varphi + \frac{\partial w}{\partial x}\right) + \frac{z}{5}\frac{\partial^2 \varphi}{\partial x^2} \\
&+\frac{z^3}{5} c_1\left(-\frac{\partial^2 \varphi}{\partial x^2} + \frac{\partial^3 w}{\partial x^3}\right) \\
&\eta_{322}^{(1)} = \eta_{232}^{(1)} = \eta_{223}^{(1)} = \frac{2}{5} c_1 z^2\left(-\frac{\partial \varphi}{\partial x} + \frac{\partial^2 w}{\partial x^2}\right) \\
&-\frac{1}{15}\left(-2\frac{\partial \varphi}{\partial x} + \frac{\partial^2 w}{\partial x^2}\right)
\end{aligned} \tag{25}$$

By substituting equations 21 and 23 into equation 10 the non - zero symmetric rotation gradient tensor can be written as:

$$\begin{aligned}
&\chi_{xy} = \chi_{yx} = -\frac{1}{4}\left(\frac{\partial^2 w}{\partial x^2} + \frac{\partial \varphi}{\partial x}\right) + \frac{3}{4} c_1 z^2\left(-\frac{\partial^2 w}{\partial x^2} + \frac{\partial \varphi}{\partial x}\right) \\
&\chi_{yz} = \chi_{yz} = -\frac{3}{2} c_1 z\left(\frac{\partial w}{\partial x} - \varphi\right)
\end{aligned} \tag{26}$$

The higher-order stresses for SVCS can be attained by substituting equations (23 -26) into equations (13-15):

$$\begin{aligned}
&\begin{Bmatrix} \tau_{111}^{(1)} \\ \tau_{111}^{*(1)} \end{Bmatrix} = -\frac{4}{5}\begin{Bmatrix} \mu l_1^2 \\ \mu^* l_1^{*2} \end{Bmatrix} z\frac{\partial^2 \varphi}{\partial x^2} - \frac{4}{5}\begin{Bmatrix} \mu l_1^2 \\ \mu^* l_1^{*2} \end{Bmatrix} c_1 z^3\left(-\frac{\partial^2 \varphi}{\partial x^2} + \frac{\partial^3 w}{\partial x^3}\right) \\
&+\frac{12}{5}\begin{Bmatrix} \mu l_1^2 \\ \mu^* l_1^{*2} \end{Bmatrix} c_1 z\left(-\varphi + \frac{\partial w}{\partial x}\right) \\
&\begin{Bmatrix} \tau_{313}^{(1)} \\ \tau_{313}^{*(1)} \end{Bmatrix} = \begin{Bmatrix} \tau_{331}^{(1)} \\ \tau_{331}^{*(1)} \end{Bmatrix} = \begin{Bmatrix} \tau_{133}^{(1)} \\ \tau_{133}^{*(1)} \end{Bmatrix} = \\
&-\frac{16}{5}\begin{Bmatrix} \mu l_1^2 \\ \mu^* l_1^{*2} \end{Bmatrix} c_1 z\left(-\varphi + \frac{\partial w}{\partial x}\right) \\
&+\frac{2z}{5}\begin{Bmatrix} \mu l_1^2 \\ \mu^* l_1^{*2} \end{Bmatrix}\frac{\partial^2 \varphi}{\partial x^2} + \frac{2z^3}{5}\begin{Bmatrix} \mu l_1^2 \\ \mu^* l_1^{*2} \end{Bmatrix} c_1\left(-\frac{\partial^2 \varphi}{\partial x^2} + \frac{\partial^3 w}{\partial x^3}\right) \\
&\begin{Bmatrix} \tau_{333}^{(1)} \\ \tau_{333}^{*(1)} \end{Bmatrix} = \frac{4}{5}\begin{Bmatrix} \mu l_1^2 \\ \mu^* l_1^{*2} \end{Bmatrix}\frac{\partial \varphi}{\partial x} - \frac{2}{5}\begin{Bmatrix} \mu l_1^2 \\ \mu^* l_1^{*2} \end{Bmatrix}\frac{\partial^2 w}{\partial x^2} \\
&+\frac{12}{5}\begin{Bmatrix} \mu l_1^2 \\ \mu^* l_1^{*2} \end{Bmatrix} c_1 z^2\left(-\frac{\partial \varphi}{\partial x} + \frac{\partial^2 w}{\partial x^2}\right) \\
&\begin{Bmatrix} \tau_{113}^{(1)} \\ \tau_{113}^{*(1)} \end{Bmatrix} = \begin{Bmatrix} \tau_{131}^{(1)} \\ \tau_{131}^{*(1)} \end{Bmatrix} = \begin{Bmatrix} \tau_{311}^{(1)} \\ \tau_{311}^{*(1)} \end{Bmatrix} = -\frac{16}{15}\begin{Bmatrix} \mu l_1^2 \\ \mu^* l_1^{*2} \end{Bmatrix}\frac{\partial \varphi}{\partial x} \\
&+\frac{8}{15}\begin{Bmatrix} \mu l_1^2 \\ \mu^* l_1^{*2} \end{Bmatrix}\frac{\partial^2 w}{\partial x^2} \\
&-\frac{16}{5}\begin{Bmatrix} \mu l_1^2 \\ \mu^* l_1^{*2} \end{Bmatrix} c_1 z^2\left(-\frac{\partial \varphi}{\partial x} + \frac{\partial^2 w}{\partial x^2}\right) \\
&\begin{Bmatrix} \tau_{122}^{(1)} \\ \tau_{122}^{*(1)} \end{Bmatrix} = \begin{Bmatrix} \tau_{212}^{(1)} \\ \tau_{212}^{*(1)} \end{Bmatrix} = \begin{Bmatrix} \tau_{221}^{(1)} \\ \tau_{221}^{*(1)} \end{Bmatrix} = \\
&\frac{4}{5}\begin{Bmatrix} \mu l_1^2 \\ \mu^* l_1^{*2} \end{Bmatrix} c_1 z\left(-\varphi + \frac{\partial w}{\partial x}\right) \\
&+\frac{2z}{5}\begin{Bmatrix} \mu l_1^2 \\ \mu^* l_1^{*2} \end{Bmatrix}\frac{\partial^2 \varphi}{\partial x^2} + \frac{2z^3}{5}\begin{Bmatrix} \mu l_1^2 \\ \mu^* l_1^{*2} \end{Bmatrix} c_1\left(-\frac{\partial^2 \varphi}{\partial x^2} + \frac{\partial^3 w}{\partial x^3}\right) \\
&\begin{Bmatrix} \tau_{322}^{(1)} \\ \tau_{322}^{*(1)} \end{Bmatrix} = \begin{Bmatrix} \tau_{232}^{(1)} \\ \tau_{232}^{*(1)} \end{Bmatrix} = \begin{Bmatrix} \tau_{223}^{(1)} \\ \tau_{223}^{*(1)} \end{Bmatrix} = \frac{4}{5}\begin{Bmatrix} \mu l_1^2 \\ \mu^* l_1^{*2} \end{Bmatrix} c_1 z^2\left(-\frac{\partial \varphi}{\partial x} + \frac{\partial^2 w}{\partial x^2}\right) \\
&-\frac{2}{15}\begin{Bmatrix} \mu l_1^2 \\ \mu^* l_1^{*2} \end{Bmatrix}\left(-2\frac{\partial \varphi}{\partial x} + \frac{\partial^2 w}{\partial x^2}\right)
\end{aligned} \tag{27}$$

$$
\begin{Bmatrix} m_{xy} \\ m_{xy}^* \end{Bmatrix} = \begin{Bmatrix} m_{yx} \\ m_{yx}^* \end{Bmatrix} = -\frac{1}{2}\begin{Bmatrix} \mu l_2^2 \\ \mu l_2^{*2} \end{Bmatrix}\left(\frac{\partial^2 w}{\partial x^2} + \frac{\partial \varphi}{\partial x}\right)
+\frac{3}{2}\begin{Bmatrix} \mu l_2^2 \\ \mu l_2^{*2} \end{Bmatrix} c_1 z^2 \left(-\frac{\partial^2 w}{\partial x^2} + \frac{\partial \varphi}{\partial x}\right)
$$

$$
\begin{Bmatrix} m_{yz} \\ m_{yz}^* \end{Bmatrix} = \begin{Bmatrix} m_{zy} \\ m_{zy}^* \end{Bmatrix} = -3\begin{Bmatrix} \mu l_2^2 \\ \mu l_2^{*2} \end{Bmatrix} c_1 z \left(\frac{\partial w}{\partial x} - \varphi\right) \tag{28}
$$

$$
\begin{Bmatrix} p_x \\ p_x^* \end{Bmatrix} = -2\begin{Bmatrix} \mu l_0^2 \\ \mu l_0^{*2} \end{Bmatrix} z \frac{\partial^2 \varphi}{\partial x^2} - 2\begin{Bmatrix} \mu l_0^2 \\ \mu l_0^{*2} \end{Bmatrix} c_1 z^3 \left(-\frac{\partial^2 \varphi}{\partial x^2} + \frac{\partial^3 w}{\partial x^3}\right)
$$

$$
\begin{Bmatrix} p_z \\ p_z^* \end{Bmatrix} = -2\begin{Bmatrix} \mu l_0^2 \\ \mu l_0^{*2} \end{Bmatrix} \frac{\partial \varphi}{\partial x} - 6\begin{Bmatrix} \mu l_0^2 \\ \mu l_0^{*2} \end{Bmatrix} c_1 z^2 \left(-\frac{\partial \varphi}{\partial x} + \frac{\partial^2 w}{\partial x^2}\right)
$$

The strain energy for micro – beam by substituting equations (18-28) into equation 6 is given by:

$$
\begin{aligned}
U_1 = \frac{1}{2}\int_0^L \{ & (-M^* + c_1 R^* - P_3^{*(0)} + 3c_1 P_3^{*(2)} - \frac{8}{5}T_{113}^{*(0)} + \frac{24}{5}c_1 T_{113}^{*(2)} \\
& + \frac{2}{5}T_{322}^{*(0)} - \frac{6}{5}c_1 T_{322}^{*(2)} + \frac{2}{5}T_{333}^{*(0)} - \frac{6}{5}c_1 T_{333}^{*(2)} - \frac{Y_{12}^{*(0)}}{2} \\
& + \frac{3c_1 Y_{12}^{*(2)}}{2})\left(\frac{\partial \varphi_1}{\partial x}\right) + (-Q^* + 3c_1 F^* - \frac{6}{5}c_1 T_{111}^{*(1)} + \frac{24}{5}c_1 T_{133}^{*(1)} \\
& - \frac{6}{5}c_1 T_{122}^{*(1)} + 3c_1 Y_{32}^{*(1)})(\varphi_1) + (-P_1^{*(1)} + c_1 P_1^{*(3)} - \frac{2}{5}T_{111}^{*(1)} + \frac{2}{5}c_1 T_{111}^{*(3)} \\
& + \frac{3}{5}T_{133}^{*(1)} - \frac{3}{5}c_1 T_{133}^{*(3)} + \frac{3}{5}T_{122}^{*(1)} - \frac{3}{5}c_1 T_{122}^{*(3)})\left(\frac{\partial^2 \varphi_1}{\partial x^2}\right) \\
& + (Q^* - 3c_1 F^* + \frac{6}{5}c_1 T_{111}^{*(1)} - \frac{24}{5}c_1 T_{133}^{*(1)} \\
& + \frac{6}{5}c_1 T_{122}^{*(1)} - 3c_1 Y_{32}^{*(1)})\left(\frac{\partial w_1}{\partial x}\right) + (-c_1 R^* - 3c_1 P_3^{*(2)} + \frac{4}{5}T_{113}^{*(0)} \\
& - \frac{24}{5}c_1 T_{113}^{*(2)} - \frac{3}{15}T_{322}^{*(0)} + \frac{6}{5}c_1 T_{322}^{*(2)} - \frac{1}{5}T_{333}^{*(0)} \\
& + \frac{6}{5}c_1 T_{333}^{*(2)} - \frac{Y_{12}^{*(0)}}{2} - \frac{3c_1 Y_{12}^{*(2)}}{2})\left(\frac{\partial^2 w_1}{\partial x^2}\right) \\
& + (-c_1 P_1^{(3)} - \frac{2}{5}c_1 T_{111}^{(3)} + \frac{3}{5}c_1 T_{133}^{(3)} + \frac{3}{5}c_1 T_{122}^{(3)})\left(\frac{\partial^3 w_1}{\partial x^3}\right)\}dx
\end{aligned} \tag{29}
$$

And for MEE composite micro-beams can be written as:

$$
\begin{aligned}
\begin{Bmatrix} U_0 \\ U_2 \end{Bmatrix} = \frac{1}{2}\int_0^L \{ & (-M + c_1 R - P_3^{(0)} + 3c_1 P_3^{(2)} - \frac{8}{5}T_{113}^{(0)} + \frac{24}{5}c_1 T_{113}^{(2)} \\
& + \frac{2}{5}T_{322}^{(0)} - \frac{6}{5}c_1 T_{322}^{(2)} + \frac{2}{5}T_{333}^{(0)} - \frac{6}{5}c_1 T_{333}^{(2)} - \frac{Y_{12}^{(0)}}{2} + \frac{3c_1 Y_{12}^{(2)}}{2})\left(\frac{\partial \begin{Bmatrix} \varphi_0 \\ \varphi_2 \end{Bmatrix}}{\partial x}\right) \\
& + (-Q + 3c_1 F - \frac{6}{5}c_1 T_{111}^{(1)} + \frac{24}{5}c_1 T_{133}^{(1)} - \frac{6}{5}c_1 T_{122}^{(1)} + 3c_1 Y_{32}^{(1)})\left(\begin{Bmatrix} \varphi_0 \\ \varphi_2 \end{Bmatrix}\right) \\
& + (-P_1^{(1)} + c_1 P_1^{(3)} - \frac{2}{5}T_{111}^{(1)} + \frac{2}{5}c_1 T_{111}^{(3)} + \frac{3}{5}T_{133}^{(1)} - \frac{3}{5}c_1 T_{133}^{(3)} \\
& + \frac{3}{5}T_{122}^{(1)} - \frac{3}{5}c_1 T_{122}^{(3)})\left(\frac{\partial^2 \begin{Bmatrix} \varphi_0 \\ \varphi_2 \end{Bmatrix}}{\partial x^2}\right) + (Q - 3c_1 F + \frac{6}{5}c_1 T_{111}^{(1)} \\
& - \frac{24}{5}c_1 T_{133}^{(1)} + \frac{6}{5}c_1 T_{122}^{(1)} - 3c_1 Y_{32}^{(1)})\left(\frac{\partial \begin{Bmatrix} w_0 \\ w_2 \end{Bmatrix}}{\partial x}\right) \\
& + (-c_1 R - 3c_1 P_3^{(2)} + \frac{4}{5}T_{113}^{(0)} - \frac{24}{5}c_1 T_{113}^{(2)} - \frac{3}{15}T_{322}^{(0)} + \frac{6}{5}c_1 T_{322}^{(2)} - \frac{1}{5}T_{333}^{(0)} \\
& + \frac{6}{5}c_1 T_{333}^{(2)} - \frac{Y_{12}^{(0)}}{2} - \frac{3c_1 Y_{12}^{(2)}}{2})\left(\frac{\partial^2 \begin{Bmatrix} w_0 \\ w_2 \end{Bmatrix}}{\partial x^2}\right) \\
& + (-c_1 P_1^{(3)} - \frac{2}{5}c_1 T_{111}^{(3)} + \frac{3}{5}c_1 T_{133}^{(3)} + \frac{3}{5}c_1 T_{122}^{(3)})\left(\frac{\partial^3 \begin{Bmatrix} w_0 \\ w_2 \end{Bmatrix}}{\partial x^3}\right)\}dx \\
& + \frac{1}{2}\int_0^L \int_A \{D_z\left(\beta \sin(\beta z)\begin{Bmatrix} \phi_{E0} \\ \phi_{E2} \end{Bmatrix} + \frac{2V_E}{h}\right) \\
& - D_x \cos(\beta z)\left(\frac{\partial \begin{Bmatrix} \phi_{E0} \\ \phi_{E2} \end{Bmatrix}}{\partial x}\right)\}dAdx + \frac{1}{2} \\
& \int_0^L \int_A \{B_z\left(\beta \sin(\beta z)\begin{Bmatrix} \Upsilon_{H0} \\ \Upsilon_{H2} \end{Bmatrix} + \frac{2\Omega_H}{h}\right) - B_x \cos(\beta z)\left(\frac{\partial \begin{Bmatrix} \Upsilon_{H0} \\ \Upsilon_{H2} \end{Bmatrix}}{\partial x}\right)\}dAdx
\end{aligned} \tag{30}
$$

The bending moments, couple moments, higher-order resultant forces and higher order moments for micro – beam and MEE composite micro- beams can be obtained from Appendix (A-2).

The work done by external loads

For modeling elastic medium between the beams, the Pasternak model is used. According to the Winkler and Pasternak foundations, the effects of the surrounding elastic medium on the outer beams are considered as follows [45]:

$$
F_{elastic\ medium} = (K_w w - K_g \nabla^2 w) \tag{31}
$$

If K_{wa} and K_{ga} considered for the elastic medium between MEE composite micro – beam (0) and micro- beam (1) and and considered for the elastic medium between micro – beam (1) and MEE composite micro - beam (2) the external work due to joined beams together can be written as follows:

$$
\begin{aligned}
V_{elastic\ medium} = & -\frac{1}{2}\int_0^L \left(\begin{Bmatrix} K_{wa}(w_0 - w_1) - \\ K_{ga}\nabla^2(w_0 - w_1) \end{Bmatrix}(w_0 - w_1)\right)dx \\
& -\frac{1}{2}\int_0^L \left(\left\{K_{wb}(w_1 - w_2) - K_{gb}\nabla^2(w_1 - w_2)\right\}(w_1 - w_2)\right)dx
\end{aligned} \tag{32}
$$

MEE composite micro – beams are subjected to the external electric voltage V_{Ej} and the external magnetic potential Ω_{Hj} and temperature change ΔT_{Ej}. The work done by this forces can be calculated as:

$$V_{external\ loads}=\frac{1}{2}\int_0^L\left((N_m+N_e+N_t)\left(\frac{\partial}{\partial x}w_j\right)^2\right)dx \qquad (33)$$
$$N_m=-2b\tilde{q}_{31}\Omega_{Hj},\ N_e=-2b\tilde{e}_{31}V_{Ej},\ N_t=\tilde{\beta}_1 bh\Delta T_j$$

Hamilton's principle

Hamilton's principle is employed here to achieve the equation of motion for smart micro- beam system. Therefore, this principle can be expressed as:

$$\int_{t_0}^{t_1}\delta\Pi dt=\int_{t_0}^{t_1}\delta(U_0+U_1+U_2-K_0-K_1-K_2-V_{elastic\ medium}-V_{external\ loads})dt=0 \qquad (34)$$

By calculating equation 34 and setting the coefficient of mechanical, electrical and magnetically to zero lead to the following motion equations:

$\delta\varphi_0$:

$$\begin{aligned}&\frac{\partial M}{\partial x}-c_1\frac{\partial R}{\partial x}-Q+3c_1F-\frac{\partial^2P_1^{(1)}}{\partial x^2}+c_1\frac{\partial^2P_1^{(3)}}{\partial x^2}\\&+\frac{\partial P_3^{(0)}}{\partial x}-3c_1\frac{\partial P_3^{(2)}}{\partial x}-\frac{2}{5}\frac{\partial^2T_{111}^{(1)}}{\partial x^2}-\frac{6}{5}c_1T_{111}^{(1)}+\frac{2}{5}c_1\frac{\partial^2T_{111}^{(3)}}{\partial x^2}\\&+\frac{8}{5}\frac{\partial T_{113}^{(0)}}{\partial x}-\frac{24}{5}c_1\frac{\partial T_{113}^{(2)}}{\partial x}+\frac{24}{5}c_1T_{133}^{(1)}+\frac{3}{5}\frac{\partial^2T_{133}^{(1)}}{\partial x^2}-\frac{3}{5}c_1\frac{\partial^2T_{133}^{(3)}}{\partial x^2}\\&+\frac{3}{5}\frac{\partial^2T_{122}^{(1)}}{\partial x^2}-\frac{3}{5}c_1\frac{\partial^2T_{122}^{(3)}}{\partial x^2}-\frac{6}{5}c_1T_{122}^{(1)}-\frac{2}{5}\frac{\partial T_{322}^{(0)}}{\partial x}+\\&\frac{6}{5}c_1\frac{\partial T_{322}^{(2)}}{\partial x}-\frac{2}{5}\frac{\partial T_{333}^{(0)}}{\partial x}+\frac{6}{5}c_1\frac{\partial T_{333}^{(2)}}{\partial x}+\frac{1}{2}\frac{\partial Y_{12}^{(0)}}{\partial x}+3c_1Y_{32}^{(1)}\\&-\frac{3}{2}c_1\frac{\partial Y_{12}^{(2)}}{\partial x}+c_1^2m_6\frac{\partial^2\varphi_0}{\partial t^2}-c_1^2m_6\frac{\partial^3w_0}{\partial x\partial t^2}-2c_1m_4\frac{\partial^2\varphi_0}{\partial t^2}+\\&c_1m_4\frac{\partial^3w_0}{\partial x\partial t^2}+m_2\frac{\partial^2\varphi_0}{\partial t^2}=0\end{aligned} \qquad (35)$$

δw_0 :

$$\begin{aligned}&-c_1\frac{\partial^2R}{\partial x^2}-\frac{\partial Q}{\partial x}+3c_1\frac{\partial F}{\partial x}+c_1\frac{\partial^3P_1^{(3)}}{\partial x^3}-3c_1\frac{\partial^2P_3^{(2)}}{\partial x^2}\\&-\frac{6}{5}c_1\frac{\partial T_{111}^{(1)}}{\partial x}+\frac{2}{5}c_1\frac{\partial^3T_{111}^{(3)}}{\partial x^3}+\frac{4}{5}\frac{\partial^2T_{113}^{(0)}}{\partial x^2}-\frac{24}{5}c_1\frac{\partial^2T_{113}^{(2)}}{\partial x^2}\\&+\frac{24}{5}c_1\frac{\partial T_{133}^{(1)}}{\partial x}-\frac{3}{5}c_1\frac{\partial^3T_{133}^{(3)}}{\partial x^3}-\frac{3}{5}c_1\frac{\partial^3T_{122}^{(3)}}{\partial x^3}-\frac{6}{5}c_1\frac{\partial T_{122}^{(1)}}{\partial x}\\&-\frac{1}{5}\frac{\partial^2T_{322}^{(0)}}{\partial x^2}+\frac{6}{5}c_1\frac{\partial^2T_{322}^{(2)}}{\partial x^2}-\frac{1}{5}\frac{\partial^2T_{333}^{(0)}}{\partial x^2}+\frac{6}{5}c_1\frac{\partial^2T_{333}^{(2)}}{\partial x^2}\\&-\frac{1}{2}\frac{\partial^2Y_{12}^{(0)}}{\partial x^2}+3c_1\frac{\partial Y_{32}^{(1)}}{\partial x}-\frac{3}{2}c_1\frac{\partial^2Y_{12}^{(2)}}{\partial x^2}+K_{wa}(w_0-w_1)\\&-K_{ga}\nabla^2(w_0-w_1)+(N_{m0}+N_{e0}+N_{t0})\frac{\partial^2w_0}{\partial x^2}\\&+c_1^2m_6\frac{\partial^3\varphi_0}{\partial x\partial t^2}-c_1^2m_6\frac{\partial^4w_0}{\partial x^2\partial t^2}\\&-c_1m_4\frac{\partial^3\varphi_0}{\partial x\partial t^2}+m_0\frac{\partial^2w_0}{\partial t^2}=0\end{aligned} \qquad (36)$$

$\delta\phi_{E0}$:

$$\int_A\left(\frac{\partial D_x}{\partial x}\cos(\beta z)+D_z\beta\sin(\beta z)\right)dA=0 \qquad (37)$$

$\delta\Upsilon_{H0}$:

$$\int_A\left(\frac{\partial B_x}{\partial x}\cos(\beta z)+B_z\beta\sin(\beta z)\right)dA=0 \qquad (38)$$

$\delta\varphi_1$:

$$\begin{aligned}&\frac{\partial M^*}{\partial x}-c_1\frac{\partial R^*}{\partial x}-Q^*+3c_1F^*-\frac{\partial^2P_1^{*(1)}}{\partial x^2}+c_1\frac{\partial^2P_1^{*(3)}}{\partial x^2}+\frac{\partial P_3^{*(0)}}{\partial x}\\&-3c_1\frac{\partial P_3^{*(2)}}{\partial x}-\frac{2}{5}\frac{\partial^2T_{111}^{*(1)}}{\partial x^2}-\frac{6}{5}c_1T_{111}^{*(1)}+\frac{2}{5}c_1\frac{\partial^2T_{111}^{*(3)}}{\partial x^2}+\frac{8}{5}\frac{\partial T_{113}^{*(0)}}{\partial x}\\&-\frac{24}{5}c_1\frac{\partial T_{113}^{*(2)}}{\partial x}+\frac{24}{5}c_1T_{133}^{*(1)}+\frac{3}{5}\frac{\partial^2T_{133}^{*(1)}}{\partial x^2}-\frac{3}{5}c_1\frac{\partial^2T_{133}^{*(3)}}{\partial x^2}+\frac{3}{5}\frac{\partial^2T_{122}^{*(1)}}{\partial x^2}\\&-\frac{3}{5}c_1\frac{\partial^2T_{122}^{*(3)}}{\partial x^2}-\frac{6}{5}c_1T_{122}^{*(1)}-\frac{2}{5}\frac{\partial T_{322}^{*(0)}}{\partial x}+\frac{6}{5}c_1\frac{\partial T_{322}^{*(2)}}{\partial x}-\frac{2}{5}\frac{\partial T_{333}^{*(0)}}{\partial x}\\&+\frac{6}{5}c_1\frac{\partial T_{333}^{*(2)}}{\partial x}+\frac{1}{2}\frac{\partial Y_{12}^{*(0)}}{\partial x}+3c_1Y_{32}^{*(1)}-\frac{3}{2}c_1\frac{\partial Y_{12}^{*(2)}}{\partial x}+c_1^2m_6^*\frac{\partial^2\varphi_1}{\partial t^2}\\&-c_1^2m_6^*\frac{\partial^3w_1}{\partial x\partial t^2}-2c_1m_4^*\frac{\partial^2\varphi_1}{\partial t^2}+c_1m_4^*\frac{\partial^3w_1}{\partial x\partial t^2}+m_2^*\frac{\partial^2\varphi_1}{\partial t^2}=0\end{aligned} \qquad (39)$$

$\delta w_1:$

$$\begin{aligned}
&-c_1\frac{\partial^2 R^*}{\partial x^2}-\frac{\partial Q^*}{\partial x}+3c_1\frac{\partial F^*}{\partial x}+c_1\frac{\partial^3 P_1^{*(3)}}{\partial x^3}-3c_1\frac{\partial^2 P_3^{*(2)}}{\partial x^2}\\
&-\frac{6}{5}c_1\frac{\partial T_{111}^{*(1)}}{\partial x}+\frac{2}{5}c_1\frac{\partial^3 T_{111}^{*(3)}}{\partial x^3}+\frac{4}{5}\frac{\partial^2 T_{113}^{*(0)}}{\partial x^2}-\frac{24}{5}c_1\frac{\partial^2 T_{113}^{*(2)}}{\partial x^2}\\
&+\frac{24}{5}c_1\frac{\partial T_{133}^{*(1)}}{\partial x}-\frac{3}{5}c_1\frac{\partial^3 T_{133}^{*(3)}}{\partial x^3}-\frac{3}{5}c_1\frac{\partial^3 T_{122}^{*(3)}}{\partial x^3}-\frac{6}{5}c_1\frac{\partial T_{122}^{*(1)}}{\partial x}\\
&-\frac{1}{5}\frac{\partial^2 T_{322}^{*(0)}}{\partial x^2}+\frac{6}{5}c_1\frac{\partial^2 T_{322}^{*(2)}}{\partial x^2}-\frac{1}{5}\frac{\partial^2 T_{333}^{*(0)}}{\partial x^2}+\frac{6}{5}c_1\frac{\partial^2 T_{333}^{*(2)}}{\partial x^2}\\
&-\frac{1}{2}\frac{\partial^2 Y_{12}^{*(0)}}{\partial x^2}+3c_1\frac{\partial Y_{32}^{*(1)}}{\partial x}-\frac{3}{2}c_1\frac{\partial^2 Y_{12}^{*(2)}}{\partial x^2}-K_{wa}(w_0-w_1)\\
&+K_{ga}\nabla^2(w_0-w_1)+K_{wb}(w_1-w_2)-K_{gb}\nabla^2(w_1-w_2)\\
&+c_1^2 m_6^*\frac{\partial^3\varphi_1}{\partial x\,\partial t^2}-c_1^2 m_6^*\frac{\partial^4 w_1}{\partial x^2\partial t^2}-c_1 m_4^*\frac{\partial^3\varphi_1}{\partial x\,\partial t^2}+m_0^*\frac{\partial^2 w_1}{\partial t^2}=0
\end{aligned}\tag{40}$$

$\delta\varphi_2:$

$$\begin{aligned}
&\frac{\partial M}{\partial x}-c_1\frac{\partial R}{\partial x}-Q+3c_1F-\frac{\partial^2 P_1^{(1)}}{\partial x^2}+c_1\frac{\partial^2 P_1^{(3)}}{\partial x^2}+\frac{\partial P_3^{(0)}}{\partial x}\\
&-3c_1\frac{\partial P_3^{(2)}}{\partial x}-\frac{2}{5}\frac{\partial^2 T_{111}^{(1)}}{\partial x^2}-\frac{6}{5}c_1T_{111}^{(1)}+\frac{2}{5}c_1\frac{\partial^2 T_{111}^{(3)}}{\partial x^2}+\frac{8}{5}\frac{\partial T_{113}^{(0)}}{\partial x}\\
&-\frac{24}{5}c_1\frac{\partial T_{113}^{(2)}}{\partial x}+\frac{24}{5}c_1T_{133}^{(1)}+\frac{3}{5}\frac{\partial^2 T_{133}^{(1)}}{\partial x^2}-\frac{3}{5}c_1\frac{\partial^2 T_{133}^{(3)}}{\partial x^2}+\frac{3}{5}\frac{\partial^2 T_{122}^{(1)}}{\partial x^2}\\
&-\frac{3}{5}c_1\frac{\partial^2 T_{122}^{(3)}}{\partial x^2}-\frac{6}{5}c_1T_{122}^{(1)}-\frac{2}{5}\frac{\partial T_{322}^{(0)}}{\partial x}+\frac{6}{5}c_1\frac{\partial T_{322}^{(2)}}{\partial x}-\frac{2}{5}\frac{\partial T_{333}^{(0)}}{\partial x}\\
&+\frac{6}{5}c_1\frac{\partial T_{333}^{(2)}}{\partial x}+\frac{1}{2}\frac{\partial Y_{12}^{(0)}}{\partial x}+3c_1Y_{32}^{(1)}-\frac{3}{2}c_1\frac{\partial Y_{12}^{(2)}}{\partial x}+c_1^2 m_6\frac{\partial^2\varphi_2}{\partial t^2}\\
&-c_1^2 m_6\frac{\partial^3 w_2}{\partial x\,\partial t^2}-2c_1m_4\frac{\partial^2\varphi_2}{\partial t^2}+c_1m_4\frac{\partial^3 w_2}{\partial x\,\partial t^2}+m_2\frac{\partial^2\varphi_2}{\partial t^2}=0
\end{aligned}\tag{41}$$

$\delta w_2:$

$$\begin{aligned}
&-c_1\frac{\partial^2 R}{\partial x^2}-\frac{\partial Q}{\partial x}+3c_1\frac{\partial F}{\partial x}+c_1\frac{\partial^3 P_1^{(3)}}{\partial x^3}-3c_1\frac{\partial^2 P_3^{(2)}}{\partial x^2}\\
&-\frac{6}{5}c_1\frac{\partial T_{111}^{(1)}}{\partial x}+\frac{2}{5}c_1\frac{\partial^3 T_{111}^{(3)}}{\partial x^3}+\frac{4}{5}\frac{\partial^2 T_{113}^{(0)}}{\partial x^2}-\frac{24}{5}c_1\frac{\partial^2 T_{113}^{(2)}}{\partial x^2}\\
&+\frac{24}{5}c_1\frac{\partial T_{133}^{(1)}}{\partial x}-\frac{3}{5}c_1\frac{\partial^3 T_{133}^{(3)}}{\partial x^3}-\frac{3}{5}c_1\frac{\partial^3 T_{122}^{(3)}}{\partial x^3}-\frac{6}{5}c_1\frac{\partial T_{122}^{(1)}}{\partial x}\\
&-\frac{1}{5}\frac{\partial^2 T_{322}^{(0)}}{\partial x^2}+\frac{6}{5}c_1\frac{\partial^2 T_{322}^{(2)}}{\partial x^2}-\frac{1}{5}\frac{\partial^2 T_{333}^{(0)}}{\partial x^2}+\frac{6}{5}c_1\frac{\partial^2 T_{333}^{(2)}}{\partial x^2}\\
&-\frac{1}{2}\frac{\partial^2 Y_{12}^{(0)}}{\partial x^2}+3c_1\frac{\partial Y_{32}^{(1)}}{\partial x}-\frac{3}{2}c_1\frac{\partial^2 Y_{12}^{(2)}}{\partial x^2}-K_{wb}(w_1-w_2)\\
&+K_{gb}\nabla^2(w_1-w_2)+(N_{m2}+N_{e2}+N_{t2})\frac{\partial^2 w_2}{\partial x^2}\\
&+c_1^2 m_6\frac{\partial^3\varphi_2}{\partial x\,\partial t^2}-c_1^2 m_6\frac{\partial^4 w_2}{\partial x^2\partial t^2}\\
&-c_1m_4\frac{\partial^3\varphi_2}{\partial x\,\partial t^2}+m_0\frac{\partial^2 w_2}{\partial t^2}=0
\end{aligned}\tag{42}$$

$\delta\phi_{E2}:$

$$\int_A\left(\frac{\partial D_x}{\partial x}\cos(\beta z)+D_z\beta\sin(\beta z)\right)dA=0\tag{43}$$

$\delta\Upsilon_{H2}:$

$$\int_A\left(\frac{\partial B_x}{\partial x}\cos(\beta z)+B_z\beta\sin(\beta z)\right)dA=0\tag{44}$$

By substituting equation (A-2) into equation (35-44) the following equations of motion can be expressed as:

$\delta\varphi_0:$

$$\begin{aligned}
&\{(A-6c_1I+9c_1^2J)\bar{c}_{44}+(\frac{96}{5}l_1^2+9l_2^2)c_1^2\mu I\}(\varphi_0-\frac{\partial w_0}{\partial x})\\
&+\{-(I-2c_1J+c_1^2K)\bar{c}_{11}-(2l_0^2+\frac{32}{15}l_1^2+\frac{1}{4}l_2^2)(\mu A)\\
&+(12l_0^2+\frac{88}{5}l_1^2+\frac{3}{2}l_2^2)(c_1\mu I)-(18l_0^2+24l_1^2+\frac{9}{4}l_2^2)(c_1^2\mu J)\}\\
&(\frac{\partial^2\varphi_0}{\partial x^2})+\{(c_1^2K-c_1J)\bar{c}_{11}+(\frac{16}{15}l_1^2-\frac{1}{4}l_2^2)(\mu A)\\
&-(6l_0^2+12l_1^2)(c_1\mu I)+(18l_0^2+24l_1^2+\frac{9}{4}l_2^2)(c_1^2\mu J)\}\\
&(\frac{\partial^3 w_0}{\partial x^3})+\{(2l_0^2+\frac{4}{5}l_1^2)(\mu I+c_1^2\mu K-2c_1\mu J)\}(\frac{\partial^4\varphi_0}{\partial x^4})\\
&-\{(2l_0^2+\frac{4}{5}l_1^2)(c_1^2\mu K-c_1\mu J)\}(\frac{\partial^5 w_0}{\partial x^5})\\
&+\{E_{31}^{(1)}-E_{31}^{(3)}c_{131}-3c_1E_{15}^{(2)}+E_{15}^{(0)}\}(\frac{\partial\phi_{E0}}{\partial x})\\
&+\{Q_{31}^{(1)}-c_1Q_{31}^{(3)}-3c_1Q_{15}^{(2)}+Q_{15}^{(0)}\}(\frac{\partial\Upsilon_{H0}}{\partial x})\\
&+c_1^2m_6\frac{\partial^2\varphi_0}{\partial t^2}-c_1^2m_6\frac{\partial^3 w_0}{\partial x\partial t^2}-2c_1m_4\frac{\partial^2\varphi_0}{\partial t^2}\\
&+c_1m_4\frac{\partial^3 w_0}{\partial x\partial t^2}+m_2\frac{\partial^2\varphi_0}{\partial t^2}=0
\end{aligned}\tag{45}$$

$\delta w_0:$

$$\begin{aligned}
&\{(A-6c_1I+9c_1^2J)\bar{c}_{44}+(\frac{96}{5}l_1^2+9l_2^2)c_1^2\mu I\}(\frac{\partial\varphi_0}{\partial x}-\frac{\partial^2 w_0}{\partial x^2})\\
&+\{(c_1J-c_1^2K)\bar{c}_{11}+(-\frac{16}{15}l_1^2+\frac{1}{4}l_2^2)(\mu A)\\
&+(6l_0^2+12l_1^2)(c_1\mu I)-(18l_0^2+24l_1^2+\frac{9}{4}l_2^2)(c_1^2\mu J)\}(\frac{\partial^3\varphi_0}{\partial x^3})\\
&+\{(c_1^2K)\bar{c}_{11}+(\frac{8}{15}l_1^2+\frac{1}{4}l_2^2)(\mu A)+(\frac{3}{2}l_2^2-\frac{32}{5}l_1^2)(c_1\mu I)\\
&+(18l_0^2+24l_1^2+\frac{9}{4}l_2^2)(c_1^2\mu J)\}(\frac{\partial^4 w_0}{\partial x^4})+(N_{m0}+N_{e0}+N_{t0})\frac{\partial^2 w_0}{\partial x^2}\\
&+\{(2l_0^2+\frac{4}{5}l_1^2)(c_1^2\mu K-c_1\mu J)\}(\frac{\partial^5\varphi_0}{\partial x^5})-\{(2l_0^2+\frac{4}{5}l_1^2)(c_1^2\mu K)\}\\
&(\frac{\partial^6 w_0}{\partial x^6})+\{-c_1E_{31}^{(3)}-3c_1E_{15}^{(2)}+E_{15}^{(0)}\}(\frac{\partial^2\phi_{E0}}{\partial x^2})\\
&+\{-c_1Q_{31}^{(3)}-3c_1Q_{15}^{(2)}+Q_{15}^{(0)}\}(\frac{\partial^2\Upsilon_{H0}}{\partial x^2})+K_{wa}(w_0-w_1)\\
&-K_{ga}\nabla^2(w_0-w_1)+c_1^2m_6\frac{\partial^3\varphi_0}{\partial x\partial t^2}\\
&-c_1^2m_6\frac{\partial^4 w_0}{\partial x^2\partial t^2}-c_1m_4\frac{\partial^3\varphi_0}{\partial x\partial t^2}+m_0\frac{\partial^2 w_0}{\partial t^2}=0
\end{aligned}\tag{46}$$

$\delta\phi_{E0}:$

$$\begin{aligned}
&-E_{31}^{(1)}\frac{\partial\varphi_0}{\partial x}-(3c_1E_{15}^{(2)}+c_1E_{31}^{(3)}-E_{15}^{(0)})(\frac{\partial^2 w_0}{\partial x^2}-\frac{\partial\varphi_0}{\partial x})\\
&+X_{11}\frac{\partial^2\phi_{E0}}{\partial x^2}+Y_{11}\frac{\partial^2\Upsilon_{H0}}{\partial x^2}-X_{33}\phi_{E0}-Y_{33}\Upsilon_{H0}=0
\end{aligned}\tag{47}$$

$\delta\Upsilon_{H0}:$

$$\begin{aligned}
&-Q_{31}^{(1)}\frac{\partial\varphi_0}{\partial x}-(3c_1Q_{15}^{(2)}+c_1Q_{31}^{(2)}-Q_{15}^{(0)})(\frac{\partial^2 w_0}{\partial x^2}-\frac{\partial\varphi_0}{\partial x})\\
&+Y_{11}\frac{\partial^2\phi_{E0}}{\partial x^2}+T_{11}\frac{\partial^2\Upsilon_{H0}}{\partial x^2}-Y_{33}\phi_{E0}-T_{33}\Upsilon_{H0}=0
\end{aligned}\tag{48}$$

$\delta\varphi_1:$

$$\begin{aligned}
&\{(A^*-6c_1I^*+9c_1^2J^*)\overline{c}_{44}^*+(\frac{96}{5}l_1^{*2}+9l_2^{*2})c_1^2\mu^*I^*\}(\varphi_1-\frac{\partial w_1}{\partial x})\\
&+\{-(I^*-2c_1J^*+c_1^2K^*)\overline{c}_{11}^*-(2l_0^{*2}+\frac{32}{15}l_1^{*2}+\frac{1}{4}l_2^{*2})(\mu^*A^*)\\
&+(12l_0^{*2}+\frac{88}{5}l_1^{*2}+\frac{3}{2}l_2^{*2})(c_1\mu^*I^*)-(18l_0^{*2}+24l_1^{*2}+\frac{9}{4}l_2^{*2})(c_1^2\mu^*J^*)\}\\
&(\frac{\partial^2\varphi_1}{\partial x^2})+\{(c_1^2K^*-c_1J^*)\overline{c}_{11}^*+(\frac{16}{15}l_1^{*2}-\frac{1}{4}l_2^{*2})(\mu^*A^*)-(6l_0^{*2}+12l_1^{*2})\\
&(c_1\mu^*I^*)+(18l_0^{*2}+24l_1^{*2}+\frac{9}{4}l_2^{*2})(c_1^2\mu^*J^*)\}(\frac{\partial^3 w_1}{\partial x^3})\\
&+\{(2l_0^{*2}+\frac{4}{5}l_1^{*2})(\mu^*I^*+c_1^2\mu^*K^*-2c_1\mu^*J^*)\}(\frac{\partial^4\varphi_1}{\partial x^4})-\{(2l_0^{*2}+\frac{4}{5}l_1^{*2})\\
&(c_1^2\mu^*K^*-c_1\mu^*J^*)\}(\frac{\partial^5 w_1}{\partial x^5})c_1^2m_6^*\frac{\partial^2\varphi_1}{\partial t^2}-c_1^2m_6^*\frac{\partial^3 w_1}{\partial x\partial t^2}-2c_1m_4^*\frac{\partial^2\varphi_1}{\partial t^2}+\\
&c_1m_4^*\frac{\partial^3 w_1}{\partial x\partial t^2}+m_2^*\frac{\partial^2\varphi_1}{\partial t^2}=0
\end{aligned}\tag{49}$$

$\delta w_1:$

$$\begin{aligned}
&(\frac{96}{5}l_1^{*2}+9l_2^{*2})c_1^2\mu^*I^*\}(\frac{\partial\varphi_1}{\partial x}-\frac{\partial^2 w_1}{\partial x^2})\\
&\{(A^*-6c_1I^*+9c_1^2J^*)\overline{c}_{44}^*+\{(c_1J^*-c_1^2K^*)\overline{c}_{11}^*\\
&+(-\frac{16}{15}l_1^{*2}+\frac{1}{4}l_2^{*2})(\mu^*A^*)+(6l_0^{*2}+12l_1^{*2})(c_1\mu^*I^*)\\
&-(18l_0^{*2}+24l_1^{*2}+\frac{9}{4}l_2^{*2})(c_1^2\mu^*J^*)\}(\frac{\partial^3\varphi_1}{\partial x^3})\\
&+\{(c_1^2K^*)\overline{c}_{11}^*+(\frac{8}{15}l_1^{*2}+\frac{1}{4}l_2^{*2})(\mu^*A^*)\\
&+(\frac{3}{2}l_2^{*2}-\frac{32}{5}l_1^{*2})(c_1\mu^*I^*)\\
&+(18l_0^{*2}+24l_1^{*2}+\frac{9}{4}l_2^{*2})(c_1^2\mu^*J^*)\}(\frac{\partial^4 w_1}{\partial x^4})+\\
&+\{(2l_0^{*2}+\frac{4}{5}l_1^{*2})(c_1^2\mu^*K^*-c_1\mu^*J^*)\}(\frac{\partial^5\varphi_1}{\partial x^5})\\
&-\{(2l_0^{*2}+\frac{4}{5}l_1^{*2})(c_1^2\mu^*K^*)\}(\frac{\partial^6 w_1}{\partial x^6})-K_{wa}(w_0-w_1)\\
&+K_{ga}\nabla^2(w_0-w_1)+K_{wb}(w_1-w_2)-K_{gb}\nabla^2(w_1-w_2)\\
&+c_1^2m_6^*\frac{\partial^3\varphi_1}{\partial x\,\partial t^2}-c_1^2m_6^*\frac{\partial^4 w_1}{\partial x^2\partial t^2}-c_1m_4^*\frac{\partial^3\varphi_1}{\partial x\,\partial t^2}+m_0^*\frac{\partial^2 w_1}{\partial t^2}=0
\end{aligned}\tag{50}$$

$\delta\varphi_2:$

$$\begin{aligned}
&\{(A-6c_1I+9c_1^2J)\overline{c}_{44}+(\frac{96}{5}l_1^2+9l_2^2)c_1^2\mu I\}(\varphi_2-\frac{\partial w_2}{\partial x})\\
&+\{-(I-2c_1J+c_1^2K)\overline{c}_{11}-(2l_0^2+\frac{32}{15}l_1^2+\frac{1}{4}l_2^2)(\mu A)\\
&+(12l_0^2+\frac{88}{5}l_1^2+\frac{3}{2}l_2^2)(c_1\mu I)\\
&-(18l_0^2+24l_1^2+\frac{9}{4}l_2^2)(c_1^2\mu J)\}(\frac{\partial^2\varphi_2}{\partial x^2})\\
&+\{(c_1^2K-c_1J)\overline{c}_{11}+(\frac{16}{15}l_1^2-\frac{1}{4}l_2^2)(\mu A)-(6l_0^2+12l_1^2)(c_1\mu I)\\
&+(18l_0^2+24l_1^2+\frac{9}{4}l_2^2)(c_1^2\mu J)\}(\frac{\partial^3 w_2}{\partial x^3})\\
&+\{(2l_0^2+\frac{4}{5}l_1^2)(\mu I+c_1^2\mu K-2c_1\mu J)\}(\frac{\partial^4\varphi_2}{\partial x^4})\\
&-\{(2l_0^2+\frac{4}{5}l_1^2)(c_1^2\mu K-c_1\mu J)\}(\frac{\partial^5 w_2}{\partial x^5})\\
&+\{E_{31}^{(1)}-E_{31}^{(3)}c_{131}-3c_1E_{15}^{(2)}+E_{15}^{(0)}\}(\frac{\partial\phi_{E2}}{\partial x})\\
&+\{Q_{31}^{(1)}-c_1Q_{31}^{(3)}-3c_1Q_{15}^{(2)}+Q_{15}^{(0)}\}(\frac{\partial\Upsilon_{H2}}{\partial x})+c_1^2m_6\frac{\partial^2\varphi_2}{\partial t^2}\\
&-c_1^2m_6\frac{\partial^3 w_2}{\partial x\,\partial t^2}-2c_1m_4\frac{\partial^2\varphi_2}{\partial t^2}+c_1m_4\frac{\partial^3 w_2}{\partial x\,\partial t^2}+m_2\frac{\partial^2\varphi_2}{\partial t^2}=0
\end{aligned}\tag{51}$$

$\delta w_2:$

$$\begin{aligned}
&\{(A-6c_1I+9c_1^2J)\overline{c}_{44}+(\frac{96}{5}l_1^2+9l_2^2)c_1^2\mu I\}(\frac{\partial\varphi_2}{\partial x}-\frac{\partial^2 w_2}{\partial x^2})\\
&+\{(c_1J-c_1^2K)\overline{c}_{11}+(-\frac{16}{15}l_1^2+\frac{1}{4}l_2^2)(\mu A)\\
&+(6l_0^2+12l_1^2)(c_1\mu I)-(18l_0^2+24l_1^2+\frac{9}{4}l_2^2)(c_1^2\mu J)\}(\frac{\partial^3\varphi_2}{\partial x^3})\\
&+\{(c_1^2K)\overline{c}_{11}+(\frac{8}{15}l_1^2+\frac{1}{4}l_2^2)(\mu A)+(\frac{3}{2}l_2^2-\frac{32}{5}l_1^2)(c_1\mu I)\\
&+(18l_0^2+24l_1^2+\frac{9}{4}l_2^2)(c_1^2\mu J)\}(\frac{\partial^4 w_2}{\partial x^4})\\
&+(N_{m2}+N_{e2}+N_{t2})\frac{\partial^2 w_2}{\partial x^2}-\{(2l_0^2+\frac{4}{5}l_1^2)(c_1^2\mu K)\}(\frac{\partial^6 w_2}{\partial x^6})\\
&+\{(2l_0^2+\frac{4}{5}l_1^2)(c_1^2\mu K-c_1\mu J)\}(\frac{\partial^5\varphi_2}{\partial x^5})\\
&+\{-c_1E_{31}^{(3)}-3c_1E_{15}^{(2)}+E_{15}^{(0)}\}(\frac{\partial^2\phi_{E2}}{\partial x^2})\\
&+\{-c_1Q_{31}^{(3)}-3c_1Q_{15}^{(2)}+Q_{15}^{(0)}\}(\frac{\partial^2\Upsilon_{H2}}{\partial x^2})\\
&-K_{wb}(w_1-w_2)+K_{gb}\nabla^2(w_1-w_2)+c_1^2m_6\frac{\partial^3\varphi_2}{\partial x\,\partial t^2}\\
&-c_1^2m_6\frac{\partial^4 w_2}{\partial x^2\partial t^2}-c_1m_4\frac{\partial^3\varphi_2}{\partial x\,\partial t^2}+m_0\frac{\partial^2 w_2}{\partial t^2}=0
\end{aligned}\tag{52}$$

$\delta\phi_{E2}:$

$$-E_{31}^{(1)}\frac{\partial\varphi_2}{\partial x}-(3c_1E_{15}^{(2)}+c_1E_{31}^{(3)}-E_{15}^{(0)})(\frac{\partial^2 w_2}{\partial x^2}-\frac{\partial\varphi_2}{\partial x})$$
$$+X_{11}\frac{\partial^2\phi_{E2}}{\partial x^2}+Y_{11}\frac{\partial^2\Upsilon_{H2}}{\partial x^2}-X_{33}\phi_{E2}-Y_{33}\Upsilon_{H2}=0 \qquad (53)$$

$\delta\Upsilon_{H2}:$

$$-Q_{31}^{(1)}\frac{\partial\varphi_2}{\partial x}-(3c_1Q_{15}^{(2)}+c_1Q_{31}^{(2)}-Q_{15}^{(0)})(\frac{\partial^2 w_2}{\partial x^2}-\frac{\partial\varphi_2}{\partial x})$$
$$+Y_{11}\frac{\partial^2\phi_{E2}}{\partial x^2}+T_{11}\frac{\partial^2\Upsilon_{H2}}{\partial x^2}-Y_{33}\phi_{E2}-T_{33}\Upsilon_{H2}=0 \qquad (54)$$

Non-dimensional form of motion equations

By introducing the dimensionless quantities that represented at Appendix (A-3), the motion equations can be obtained in the following dimensionless form:

$\delta\Psi_0:$

$$\{(a_{44}-6i_{55}+9j_{55})+(\frac{96}{5}\ell_1^2+9\ell_2^2)\frac{i_{66}}{\eta^2}\}(\Psi_0-\frac{1}{\eta}\frac{\partial W_0}{\partial X})$$
$$+\{-(i_{22}-2j_{22}+k_{33})-(2\ell_0^2+\frac{32}{15}\ell_1^2+\frac{1}{4}\ell_2^2)a_{55}$$
$$+(12\ell_0^2+\frac{88}{5}\ell_1^2+\frac{3}{2}\ell_2^2)i_{44}+\{(k_{33}-j_{22})+(\frac{16}{15}\ell_1^2-\frac{1}{4}\ell_2^2)a_{55}$$
$$-(18\ell_0^2+24\ell_1^2+\frac{9}{4}\ell_2^2)j_{44}\}(\frac{1}{\eta^2}\frac{\partial^2\Psi_0}{\partial X^2})$$
$$-(6\ell_0^2+12\ell_1^2)i_{44}+(18\ell_0^2+24\ell_1^2+\frac{9}{4}\ell_2^2)j_{44}\}(\frac{1}{\eta^3}\frac{\partial^3 W_0}{\partial X^3})$$
$$+\{(2\ell_0^2+\frac{4}{5}\ell_1^2)(i_{33}+k_{22}-2j_{33})\}(\frac{1}{\eta^4}\frac{\partial^4\Psi_0}{\partial X^4})$$
$$-\{(2\ell_0^2+\frac{4}{5}\ell_1^2)(k_{22}-j_{33})\}(\frac{1}{\eta^5}\frac{\partial^5 W_0}{\partial X^5})$$
$$+\{E_{31}-F_{31}\hat{c}_1-3\hat{c}_1F_{15}+E_{15}\}(\frac{1}{\eta}\frac{\partial\Phi_{E0}}{\partial X})$$
$$+\{Q_{31}-\hat{c}_1G_{31}-3\hat{c}_1G_{15}+Q_{15}\}(\frac{1}{\eta}\frac{\partial\Theta_{H0}}{\partial X})$$
$$+(\hat{c}_1^2I_{166}-2\hat{c}_1I_{144}+I_{122})(\frac{1}{\eta^2}\frac{\partial^2\Psi_0}{\partial\tau^2})$$
$$+(\hat{c}_1I_{144}-\hat{c}_1^2I_{166})(\frac{1}{\eta^3}\frac{\partial^3 W_0}{\partial X\,\partial\tau^2})=0 \qquad (55)$$

$\delta W_0:$

$$\{(a_{44}-6i_{55}+9j_{55})+(\frac{96}{5}\ell_1^2+9\ell_2^2)\frac{i_{66}}{\eta^2}\}$$
$$(\frac{\partial\Psi_0}{\partial X}-\frac{1}{\eta}\frac{\partial^2 W_0}{\partial X^2})+\{(j_{22}-k_{33})+(-\frac{16}{15}\ell_1^2+\frac{1}{4}\ell_2^2)a_{55}$$
$$+(6\ell_0^2+12\ell_1^2)i_{44}-(18\ell_0^2+24\ell_1^2+\frac{9}{4}\ell_2^2)j_{44}\}(\frac{1}{\eta^2}\frac{\partial^3\Psi_0}{\partial X^3})$$
$$+\{k_{33}+(\frac{8}{15}\ell_1^2+\frac{1}{4}\ell_2^2)a_{55}+(\frac{3}{2}\ell_2^2-\frac{32}{5}\ell_1^2)i_{44}+$$
$$(18\ell_0^2+24\ell_1^2+\frac{9}{4}\ell_2^2)j_{44}\}(\frac{1}{\eta^3}\frac{\partial^4 W_0}{\partial X^4})+(\bar{N}_{m0}+\bar{N}_{e0}+\bar{N}_{t0})$$
$$(\frac{1}{\eta})\frac{\partial^2 W_0}{\partial x^2}+\{(2\ell_0^2+\frac{4}{5}\ell_1^2)(k_{22}-j_{33})\}(\frac{1}{\eta^4}\frac{\partial^5\Psi_0}{\partial X^5})$$
$$-\{(2\ell_0^2+\frac{4}{5}\ell_1^2)(k_{22})\}(\frac{1}{\eta^5}\frac{\partial^6 W_0}{\partial X^6})+\{-\hat{c}_1F_{31}-3\hat{c}_1F_{15}+E_{15}\}$$
$$(\frac{1}{\eta}\frac{\partial^2\Phi_{E0}}{\partial X^2})+\{-\hat{c}_1G_{31}-3\hat{c}_1G_{15}+Q_{15}\}(\frac{1}{\eta}\frac{\partial^2\Theta_{H0}}{\partial X^2})$$
$$+\frac{k_{wa}}{\eta}(W_0-W_1)-\frac{K_{ga}}{\eta}\nabla^2(W_0-W_1)$$
$$+(\hat{c}_1^2I_{166}-\hat{c}_1I_{144})(\frac{1}{\eta^2}\frac{\partial^3\Psi_0}{\partial X\partial\tau^2})-\frac{\hat{c}_1^2I_{166}}{\eta^3}\frac{\partial^4 W_0}{\partial X^2\partial\tau^2}+\frac{I_{100}}{\eta}\frac{\partial^2 W_0}{\partial\tau^2}=0 \qquad (56)$$

$\delta\Phi_{E0}:$

$$-E_{31}\eta\frac{\partial\Psi_0}{\partial X}-(3\hat{c}_1F_{15}+\hat{c}_1F_{31}-E_{15})(\frac{\partial^2 W_0}{\partial X^2}-\eta\frac{\partial\Psi_0}{\partial X})$$
$$+\hat{X}_{11}\frac{\partial^2\Phi_{E0}}{\partial X^2}+\hat{Y}_{11}\frac{\partial^2\Theta_{H0}}{\partial X^2}-\hat{X}_{33}\eta^2\Phi_{E0}-\hat{Y}_{33}\eta^2\Theta_{H0}=0 \qquad (57)$$

$\delta\Theta_{H0}:$

$$-Q_{31}\eta\frac{\partial\Psi_0}{\partial X}-(3\hat{c}_1G_{15}+\hat{c}_1G_{31}-Q_{15})(\frac{\partial^2 W_0}{\partial X^2}-\eta\frac{\partial\Psi_0}{\partial X})$$
$$+\hat{Y}_{11}\frac{\partial^2\Phi_{E0}}{\partial X^2}+\hat{T}_{11}\frac{\partial^2\Theta_{H0}}{\partial X^2}-\hat{Y}_{33}\eta^2\Phi_{E0}-\hat{T}_{33}\eta^2\Theta_{H0}=0 \qquad (58)$$

$\delta\Psi_1:$

$$\{(a_{44}^*-6i_{55}^*+9j_{55}^*)+(\frac{96}{5}\ell_1^{*2}+9\ell_2^{*2})\frac{i_{66}^*}{\eta^2}\}(\Psi_1-\frac{1}{\eta}\frac{\partial W_1}{\partial X})$$
$$+\{-(i_{22}^*-2j_{22}^*+k_{33}^*)-(2\ell_0^{*2}+\frac{32}{15}\ell_1^{*2}+\frac{1}{4}\ell_2^{*2})a_{55}^*$$
$$+(12\ell_0^{*2}+\frac{88}{5}\ell_1^{*2}+\frac{3}{2}\ell_2^{*2})i_{44}^*-(18\ell_0^{*2}+24\ell_1^{*2}+\frac{9}{4}\ell_2^{*2})j_{44}^*\}(\frac{1}{\eta^2}\frac{\partial^2\Psi_1}{\partial X^2})$$
$$+\{(k_{33}^*-j_{22}^*)+(\frac{16}{15}\ell_1^{*2}-\frac{1}{4}\ell_2^{*2})a_{55}^*-(6\ell_0^{*2}+12\ell_1^{*2})i_{44}^*$$
$$+(18\ell_0^{*2}+24\ell_1^{*2}+\frac{9}{4}\ell_2^{*2})j_{44}^*\}(\frac{1}{\eta^3}\frac{\partial^3 W_1}{\partial X^3})$$
$$+\{(2\ell_0^{*2}+\frac{4}{5}\ell_1^{*2})(i_{33}^*+k_{22}^*-2j_{33}^*)\}(\frac{1}{\eta^4}\frac{\partial^4\Psi_1}{\partial X^4})$$
$$-\{(2\ell_0^{*2}+\frac{4}{5}\ell_1^{*2})(k_{22}^*-j_{33}^*)\}(\frac{1}{\eta^5}\frac{\partial^5 W_1}{\partial X^5})$$
$$+(\hat{c}_1^2I_{166}^*-2\hat{c}_1I_{144}^*+I_{122}^*)(\frac{1}{\eta^2}\frac{\partial^2\Psi_1}{\partial\tau^2})+$$
$$(\hat{c}_1I_{144}^*-\hat{c}_1^2I_{166}^*)(\frac{1}{\eta^3}\frac{\partial^3 W_1}{\partial X\partial\tau^2})=0 \qquad (59)$$

δW_1:

$$
\begin{aligned}
&\{(a_{44}^{*}-6i_{55}^{*}+9j_{55}^{*})+(\frac{96}{5}\ell_1^{*2}+9\ell_2^{*2})\frac{i_{66}^{*}}{\eta^2}\}(\frac{\partial \Psi_1}{\partial X}-\frac{1}{\eta}\frac{\partial^2 W_1}{\partial X^2})\\
&+\{(j_{22}^{*}-k_{33}^{*})+(-\frac{16}{15}\ell_1^{*2}+\frac{1}{4}\ell_2^{*2})a_{55}^{*}\\
&+(6\ell_0^{*2}+12\ell_1^{*2})i_{44}^{*}-(18\ell_0^{*2}+24\ell_1^{*2}+\frac{9}{4}\ell_2^{*2})j_{44}^{*}\}(\frac{1}{\eta^2}\frac{\partial^3 \Psi_1}{\partial X^3})\\
&+\{k_{33}^{*}+(\frac{8}{15}\ell_1^{*2}+\frac{1}{4}\ell_2^{*2})a_{55}^{*}+(\frac{3}{2}\ell_2^{*2}-\frac{32}{5}\ell_1^{*2})i_{44}^{*}\\
&+(18\ell_0^{*2}+24\ell_1^{*2}+\frac{9}{4}\ell_2^{*2})j_{44}^{*}\}(\frac{1}{\eta^3}\frac{\partial^4 W_1}{\partial X^4})\\
&+\{(2\ell_0^{*2}+\frac{4}{5}\ell_1^{*2})(k_{22}^{*}-j_{33}^{*})\}(\frac{1}{\eta^4}\frac{\partial^5 \Psi_1}{\partial X^5})\\
&-\{(2\ell_0^{*2}+\frac{4}{5}\ell_1^{*2})(k_{22}^{*})\}(\frac{1}{\eta^5}\frac{\partial^6 W_1}{\partial X^6})\\
&-\frac{k_{wa}}{\eta}(W_0-W_1)+\frac{k_{ga}}{\eta}\nabla^2(W_0-W_1)+\frac{k_{wb}}{\eta}(W_1-W_2)\\
&-\frac{k_{gb}}{\eta}\nabla^2(W_1-W_2)+(\hat{c}_1^2 I_{166}^{*}-\hat{c}_1 I_{144}^{*})(\frac{1}{\eta^2}\frac{\partial^3 \Psi_1}{\partial X\,\partial\tau^2})\\
&-\frac{\hat{c}_1^2 I_{166}^{*}}{\eta^3}\frac{\partial^4 W_1}{\partial X^2\partial\tau^2}+\frac{I_{100}^{*}}{\eta}\frac{\partial^2 W_1}{\partial\tau^2}=0
\end{aligned}
\tag{60}
$$

$\delta\Psi_2$:

$$
\begin{aligned}
&\{(a_{44}-6i_{55}+9j_{55})+(\frac{96}{5}\ell_1^2+9\ell_2^2)\frac{i_{66}}{\eta^2}\}(\Psi_2-\frac{1}{\eta}\frac{\partial W_2}{\partial X})\\
&+\{-(i_{22}-2j_{22}+k_{33})-(2\ell_0^2+\frac{32}{15}\ell_1^2+\frac{1}{4}\ell_2^2)a_{55}\\
&-(18\ell_0^2+24\ell_1^2+\frac{9}{4}\ell_2^2)j_{44}\}(\frac{1}{\eta^2}\frac{\partial^2 \Psi_2}{\partial X^2})\\
&+(\frac{16}{15}\ell_1^2-\frac{1}{4}\ell_2^2)a_{55}+(\hat{c}_1^2 I_{166}-2\hat{c}_1 I_{144}+I_{122})(\frac{1}{\eta^2}\frac{\partial^2\Psi_2}{\partial\tau^2})\\
&+(18\ell_0^2+24\ell_1^2+\frac{9}{4}\ell_2^2)j_{44}\}(\frac{1}{\eta^3}\frac{\partial^3 W_2}{\partial X^3})+\{(k_{33}-j_{22})\\
&+\{(2\ell_0^2+\frac{4}{5}\ell_1^2)(i_{33}+k_{22}-2j_{33})\}(\frac{1}{\eta^4}\frac{\partial^4\Psi_2}{\partial X^4})\\
&-\{(2\ell_0^2+\frac{4}{5}\ell_1^2)(k_{22}-j_{33})\}(\frac{1}{\eta^5}\frac{\partial^5 W_2}{\partial X^5})-(6\ell_0^2+12\ell_1^2)i_{44}\\
&+\{E_{31}-F_{31}\hat{c}_1-3\hat{c}_1F_{15}+E_{15}\}(\frac{1}{\eta}\frac{\partial\Phi_{E2}}{\partial X})\\
&+\{Q_{31}-\hat{c}_1G_{31}-3\hat{c}_1G_{15}+Q_{15}\}(\frac{1}{\eta}\frac{\partial\Theta_{H2}}{\partial X})\\
&+(12\ell_0^2+\frac{88}{5}\ell_1^2+\frac{3}{2}\ell_2^2)i_{44}+(\hat{c}_1 I_{144}-\hat{c}_1^2 I_{166})(\frac{1}{\eta^3}\frac{\partial^3 W_2}{\partial X\,\partial\tau^2})=0
\end{aligned}
\tag{61}
$$

δW_2:

$$
\begin{aligned}
&\{(a_{44}-6i_{55}+9j_{55})+(\frac{96}{5}\ell_1^2+9\ell_2^2)\frac{i_{66}}{\eta^2}\}(\frac{\partial\Psi_2}{\partial X}-\frac{1}{\eta}\frac{\partial^2 W_2}{\partial X^2})\\
&+\{(j_{22}-k_{33})+(-\frac{16}{15}\ell_1^2+\frac{1}{4}\ell_2^2)a_{55}\\
&+(6\ell_0^2+12\ell_1^2)i_{44}-(18\ell_0^2+24\ell_1^2+\frac{9}{4}\ell_2^2)j_{44}\}(\frac{1}{\eta^2}\frac{\partial^3\Psi_2}{\partial X^3})\\
&+\{k_{33}+(\frac{8}{15}\ell_1^2+\frac{1}{4}\ell_2^2)a_{55}+(\frac{3}{2}\ell_2^2-\frac{32}{5}\ell_1^2)i_{44}\\
&+(18\ell_0^2+24\ell_1^2+\frac{9}{4}\ell_2^2)j_{44}\}(\frac{1}{\eta^3}\frac{\partial^4 W_2}{\partial X^4})\\
&+(\bar{N}_{m2}+\bar{N}_{e2}+\bar{N}_{t2})(\frac{1}{\eta})\frac{\partial^2 W_2}{\partial x^2}\\
&+\{(2\ell_0^2+\frac{4}{5}\ell_1^2)(k_{22}-j_{33})\}(\frac{1}{\eta^4}\frac{\partial^5\Psi_2}{\partial X^5})\\
&-\{(2\ell_0^2+\frac{4}{5}\ell_1^2)(k_{22})\}(\frac{1}{\eta^5}\frac{\partial^6 W_2}{\partial X^6})\\
&+\{-\hat{c}_1F_{31}-3\hat{c}_1F_{15}+E_{15}\}(\frac{1}{\eta}\frac{\partial^2\Phi_{E2}}{\partial X^2})\\
&+\{-\hat{c}_1G_{31}-3\hat{c}_1G_{15}+Q_{15}\}(\frac{1}{\eta}\frac{\partial^2\Theta_{H2}}{\partial X^2})\\
&-\frac{k_{wb}}{\eta}(W_1-W_2)+\frac{k_{gb}}{\eta}\nabla^2(W_1-W_2)\\
&+(\hat{c}_1^2 I_{166}-\hat{c}_1 I_{144})(\frac{1}{\eta^2}\frac{\partial^3\Psi_2}{\partial X\partial\tau^2})-\frac{\hat{c}_1^2 I_{166}}{\eta^3}\frac{\partial^4 W_2}{\partial X^2\partial\tau^2}\\
&+\frac{I_{100}}{\eta}\frac{\partial^2 W_2}{\partial\tau^2}=0
\end{aligned}
\tag{62}
$$

$\delta\Phi_{E2}$:

$$
\begin{aligned}
&-E_{31}\eta\frac{\partial\Psi_2}{\partial X}-(3\hat{c}_1F_{15}+\hat{c}_1F_{31}-E_{15})(\frac{\partial^2 W_2}{\partial X^2}-\eta\frac{\partial\Psi_2}{\partial X})\\
&+\hat{X}_{11}\frac{\partial^2\Phi_{E2}}{\partial X^2}+\hat{Y}_{11}\frac{\partial^2\Theta_{H2}}{\partial X^2}-\hat{X}_{33}\eta^2\Phi_{E2}-\hat{Y}_{33}\eta^2\Theta_{H2}=0
\end{aligned}
\tag{63}
$$

$\delta\Theta_{H2}$:

$$
\begin{aligned}
&-Q_{31}\eta\frac{\partial\Psi_3}{\partial X}-(3\hat{c}_1G_{15}+\hat{c}_1G_{31}-Q_{15})(\frac{\partial^2 W_2}{\partial X^2}-\eta\frac{\partial\Psi_2}{\partial X})\\
&+\hat{Y}_{11}\frac{\partial^2\Phi_{E2}}{\partial X^2}+\hat{T}_{11}\frac{\partial^2\Theta_{H2}}{\partial X^2}-\hat{Y}_{33}\eta^2\Phi_{E2}-\hat{T}_{33}\eta^2\Theta_{H2}=0
\end{aligned}
\tag{64}
$$

The dimensionless simply supported (S-S) boundary conditions for smart micro- beam system are considered as follows:

$$
W_i=\frac{\partial\Psi_i}{\partial X}=\Phi_i=\Theta_i=0,\ \frac{\partial^2 W_i}{\partial X^2}=0\quad at\ (\mathrm{X}=0,1)\ i=0,1,2 \tag{65}
$$

SOLUTION PROCEDURE

The differential quadrature method (DQM) is employed to solve the motion equations (55–64) and the associated boundary condition (64) to determine the natural frequencies and mode shape of the smart micro- beam system. DQM transforms the differential equations into a set of analogous algebraic equations in terms of the unknown function values at the resembled points in the solution domain [46].This method is used to discretize the motion equations using the approximation of derivatives of the function f(x) by linear sums of all functional values in the domain[47,48]:

$$\left.\frac{d^p f}{dx^p}\right|_{x=x_i} = \sum_{j=1}^{N} A_{ij}^{p} f\,(\mathrm{x}_j) \quad i=1,2,...,N \tag{66}$$

The first order derivatives is obtained by following equation[49-51]:

$$\begin{aligned} C_{ij}^{(1)} &= \frac{M_1(x_i)}{(x_i - x_j)M_1(x_j)} \quad for\ i \neq j \quad i,j=1,2,...,N \\ C_{ij}^{(1)} &= -\sum_{j=1, j\neq i} C_{ij}^{1} \quad for\ i=j \quad i,j=1,2,...,N \end{aligned} \tag{67}$$

Where:

$$M\,(x_i) = \prod_{\substack{j=1 \\ j\neq i}}^{N_x} (x_i - x_j) \tag{68}$$

The pth order derivative can be obtained as follow:

$$\left[A^{(n)}\right] = \left[A^{(1)}\right]^n \tag{69}$$

For determine the unequally spaced position of the grid points the Chebyshev–Gauss–Lobatto polynomials was employed as follow [25]:

$$x_i = \frac{L}{2}\left[1-\cos\left(\frac{2i-1}{N-1}\right)\pi\right] \quad i=1,2,...,N \tag{70}$$

Applying the relationships (66) to equations (55-64), one obtains a set of linear ordinary differential equations that represented at Appendix (A-5) - (A-15). The associated boundary conditions can behandled in the same way. For boundary condition (65) can be written as:

$$\begin{aligned} & W_i = \sum_{1}^{N} A_{ij}^{(1)}\Psi_i = \Phi_{Ej} = \Theta_{Hj} = 0,\ \sum_{1}^{N} A_{ij}^{(2)} W_2 = 0 \\ & at \quad \mathrm{X}=0 \\ & W_{iN} = \sum_{1}^{N} A_{ij}^{(1)}\Psi_{iN} = \Phi_{EjN} = \Theta_{EjN} = 0,\ \sum_{1}^{N} A_{ij}^{(2)} W_{N\,2} = 0 \\ & at \quad \mathrm{X}=1 \end{aligned} \tag{71}$$

Linear ordinary differential equations together with the boundary conditions, can be expressed as the following matrix form:

$$[M]\{\ddot{q}\} + [K]\{q\} = 0 \tag{72}$$

In which shows the unknown dynamic displacement vector as:

$$\{q\} = \left\{\{W_i\}^T, \{\Psi_i\}^T, \{\Phi_i\}^T, \{\Theta_i\}^T\right\}^T \tag{73}$$

General solution of motion equations are considered as:

$$\begin{aligned} \mathrm{W}_i(x,t) &= \widehat{W}_i(X)\,\mathrm{e}^{i\omega\tau} \\ \Psi_i(x,t) &= \widehat{\Psi}_i(X)\,\mathrm{e}^{i\omega\tau} \\ \Phi_i(x,t) &= \widehat{\Phi}_i(X)\,\mathrm{e}^{i\omega\tau} \\ \Theta_i(x,t) &= \widehat{\Theta}_i(X)\,\mathrm{e}^{i\omega\tau} \end{aligned} \tag{74}$$

where $\omega = \sqrt{\frac{m_0}{A_{44}}}\Omega L$ represents the dimensionless natural frequency; $\widehat{W}_i(X)$, $\widehat{\Psi}_i(X)$, $\widehat{\Phi}_i(X)$ and $\widehat{\Theta}_i(X)$ are the components of vibration mode shape vector $\{q^*\}$. ubstituting equation 74 into equation 72 yields:

$$([\mathrm{K}] - [M]\omega^2)\{q^*\} = \{0\} \tag{75}$$

By solving equation 75, the dimensionless natural frequencies and their associated vibration mode shapes can be obtained.

NUMERICAL RESULTS

The current numerical results are given for the smart micro- beam system at (SS-SS) boundary condition. MEE numbers 0 and 2 are made of two-phase $BiTiO_3$–$CoFe_2O_4$ composites whose material properties are listed in reference [24] and [25]. Micro beam number 1 made of epoxy with the elastic modulus (E = 1.44 GPa), density (=1220) and the Poisson’s ratio (= 0.38)[52].Pasternak and Winkler constants and the other properties for MEE composite microbeams (0, 2) and microbeam (1) are considered as:

$$\begin{aligned} & \mathrm{l} = 17.6\mu m, h = 2l, b = 2h, \mathrm{L} = 10h, K_{wa} = K_{wb} = 10^{12}\left(\frac{N}{m^2}\right) \\ & , K_{ga} = K_{gb} = 10(N) \end{aligned} \tag{76}$$

It should be noted that all of represented results are based on equation 76, the data of each Table or Figure is stated under them.

(71)

The concluded results are compared with simplified analysis is represented by Wang et al. [53] on vibration of the microbeam (1) in which the MEE micro beams (0,2) are ignored. Therefore, Figure 2 shows the comparison between the obtained results for normalized frequency of present work and results obtained by Ref. [53]. It is shown that there are a good agreement between them and show similar results for classical theory (CT) $(\ell_0 = \ell_1 = \ell_2 = 0)$ modified couple stress theory (MCST) $(\ell_0 = \ell_1 = 0, = \ell_2 = l)$ and strain gradient theory (SGT) .

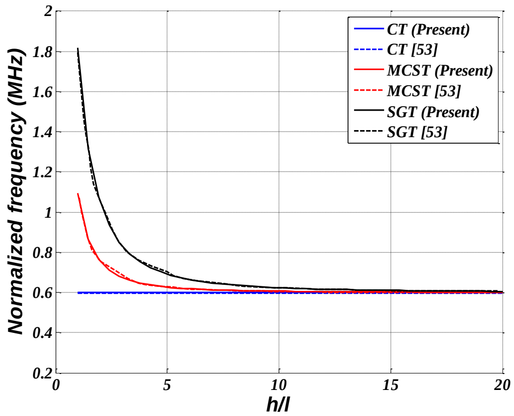

Fig. 2. Comparison present results with those obtained by Wang et al. [53]

Table 1 represents the dimensionless first three dimensionless natural frequencies of micro-beam (1) system only, MEE composite micro – beam (0) with micro-beam (1) together and smart micro – beam system (0,1,2)for different values of aspect ratio($\frac{h}{l}$) based on R – L beam model (RLBM) and Timoshenko beam model (TBM) using MSGT, MCST and CT.

The results of this Table are shown as follows:

- The dimensionless natural frequencies at each three system for MSGT are higher than for MCST and CT.
- By increasing the value of aspect ratio, dimensionless natural frequencies at (RLBM) and (TBM) for MSGT and MCST decreases and at CT is constant.
- Dimensionless natural frequencies at (RLBM) is higher than (TBM) for each three MSGT,MCST andCT and each aspect ratio.
- The smart micro – beam system have less dimensionless natural frequencies than micro-beam (1) system only and MEE composite micro – beam (0) with micro-beam (1) together.
- The micro-beam (1) system has maximum dimensionless natural frequencies.

Figure 3 shows the effect of the external magnetic potential on the dimensionless fundamental natural frequency of the smart micro- beam system based on MSGT. It is shown that by increasing the external magnetic potential on the MEE micro beams, the dimensionless natural frequency of the smart micro- beam system increases.

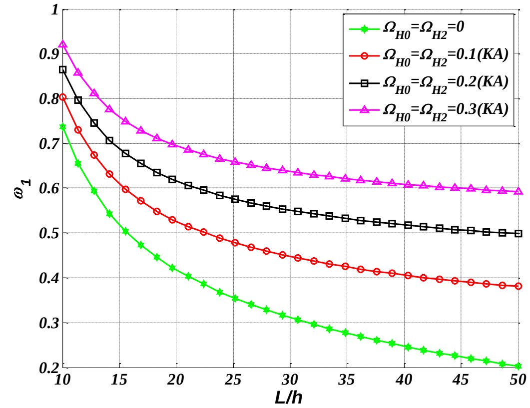

Fig. 3. The effect of external magnetic parameter on the dimensionless fundamental natural frequency based on MSGT. $(V_{E0} = V_{E2} = \Delta T_0 = \Delta T_2 = 0)$.

The effect of the external electric voltage on the dimensionless fundamental natural frequency of the smart micro- beam system based on MSGT is illustrated in Figure 4. It can be observed that the dimensionless natural frequency of the smart micro- beam system decreases with increasing the external electric voltage on the MEE micro beams. This is because that the imposed voltages brings in more reduction in the stiffness of MEE micro beams, and hence leads to lower natural frequencies of SVC system respectively. Obviously, the effect of the external electric potential is opposite to that of the external magnetic potential.

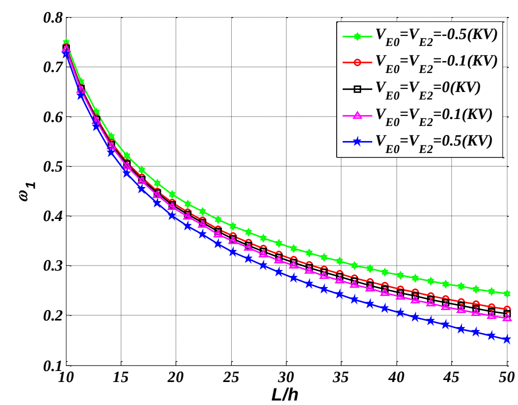

Fig. 4. The effect of external magnetic parameter on the dimensionless fundamental natural frequency based on MSGT $(\Omega_{H0} = \Omega_{H2} = \Delta T_0 = \Delta T_2 = 0)$.

Table 1

the dimensionless first three dimensionless natural frequencies of micro-beam (1) system only, MEE composite micro – beam (0) with micro-beam (1) together and smart micro – beam system (0,1,2) for different values of aspect ratio ($\frac{h}{l}$) based on R – L beam model (RLBM) and Timoshenko beam model (TBM) using MSGT, MCST and CT

Various theory	mode	(1)	(0,1)	(0,1,2)	(1)	(0,1)	(0,1,2)	(1)	(0,1)	(0,1,2)
		$h=2l$			$h=4l$			$h=6l$		
MSGT (RLBM)	1	1.1163	0.9637	0.7371	0.7861	0.6385	0.4971	0.7081	0.5577	0.4360
	2	4.3066	3.7218	2.7491	3.0317	2.4692	1.8308	2.7288	2.1556	1.6004
	3	9.2169	7.9688	5.8256	6.4749	5.2902	3.9286	5.8183	4.6133	3.4390
MSGT (TBM)	1	1.0634	0.9236	0.7159	0.7701	0.6292	0.4507	0.6974	0.5524	0.4055
	2	3.7045	3.2569	2.4030	2.8259	2.3464	1.7387	2.5882	2.0846	1.5471
	3	7.1916	6.3893	4.7047	5.6931	4.8121	3.4966	5.2695	4.3288	3.1761
MCST (RLBM)	1	0.8048	0.6574	0.5062	0.6840	0.5321	0.4143	0.6593	0.5055	0.3947
	2	3.1168	2.5539	1.8934	2.6386	2.0592	1.5297	2.5402	1.9539	1.4523
	3	6.6937	5.5039	4.0756	5.6315	4.4125	3.2893	5.4119	4.1791	3.1202
MCST (TBM)	1	0.7937	0.6518	0.5007	0.6762	0.5288	0.4094	0.6520	0.5026	0.3884
	2	2.9703	2.4769	1.8350	2.5333	2.0144	1.4958	2.4422	1.9147	1.4227
	3	6.1181	5.1936	3.8391	5.2133	4.2301	3.1469	5.0222	4.0194	2.9920
CT (RLBM)	1	0.6387	0.4832	0.3782	0.6387	0.4832	0.3782	0.6387	0.4832	0.3782
	2	2.4587	1.8653	1.3872	2.4587	1.8653	1.3872	2.4587	1.8653	1.3872
	3	5.2297	3.9824	2.9777	5.2297	3.9824	2.9777	5.2297	3.9824	2.9777
CT (TBM)	1	0.6319	0.4806	0.3580	0.6319	0.4806	0.3580	0.6319	0.4806	0.3580
	2	2.3665	1.8307	1.3610	2.3665	1.8307	1.3610	2.3665	1.8307	1.3610
	3	4.8625	3.8409	2.8371	4.8625	3.8409	2.8371	4.8625	3.8409	2.8371

"Table guide"

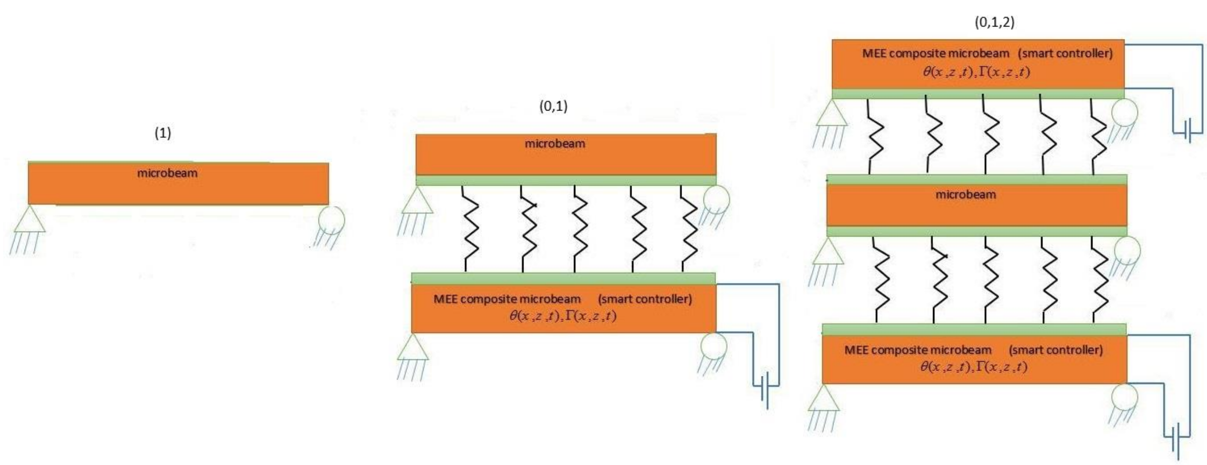

The effect of shear Pasternak constant and spring Winkler constant between microbeam(1) and MEE micro beams(0,2) versus external temperature change of MEE microbeam(0) based on MSGT are shown in Figures 5 and 6. It is concluded that the dimensionless natural frequency of smart micro-beam system increases with an increase in the spring and shear constants of elastic foundation. Considering the elastic foundation leads to increase stiffness of smart micro- beam system. In addition, it is evident that with an increase in the external temperature change of MEE microbeam (0), dimensionless natural frequency of smart micro- beam system decreases. It is due to the fact that rise the temperature gradient leads to softer structure .

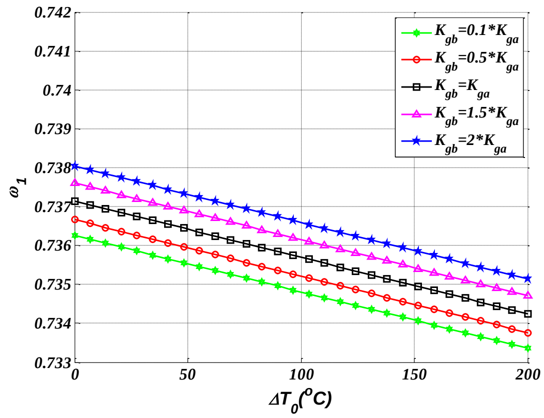

Fig. 5. The effect of shear Pasternak constant between microbeam(1) and MEE micro beams(0,2)versus external temperature change of MEE microbeam(0) based on MSGT $(\Omega_{H0} = \Omega_{H2} = V_{E0} = V_{E2} = \Delta T_2 = 0)$.

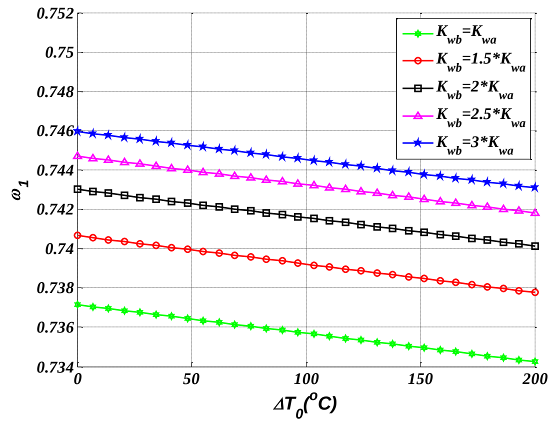

Fig. 6. The effect ofspring Winkler constant between microbeam(1) and MEE micro beams(0,2)versus external temperature change of MEE microbeam(0) based on MSGT
$(\Omega_{H0} = \Omega_{H2} = V_{E0} = V_{E2} = \Delta T_2 = 0)$.

Figures 7 and 8 depict the effect of spring and shear constants between micro-beam and MEE composite micro - beams of smart micro - beam system versus aspect ratio based on MSGT and MCST, respectively.

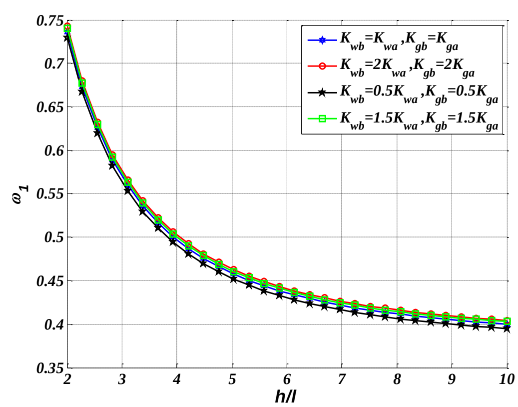

Fig. 7. The effect of different spring and shear constants between micro beams(0,1,2) versus aspect ratio based on MSGT.
$(\Delta T_0 = \Delta T_2 = \Omega_{H0} = \Omega_{H2} = V_{E0} = V_{E2} = 0)$.

It is shown that the dimensionless natural frequency increases with an increase in the spring and shear constants of elastic foundation, while the stiffness of micro-beam as well as natural frequency increases.

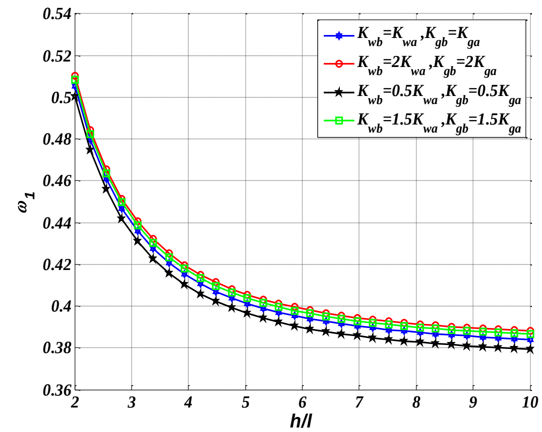

Fig. 8. The effect of external voltage on the dimensionless fundamental natural frequency versus external magnetic potential of MEE microbeam (0) based on MCST. $(\Delta T_0 = \Delta T_2 = \Omega_{H2} = 0, V_{E2} = 0.01(V))$.

Figure 9 show the effect of material length scale parameter on the dimensionless magnetic potential for micro-beam (0) based on MSGT (mode shapes 1).

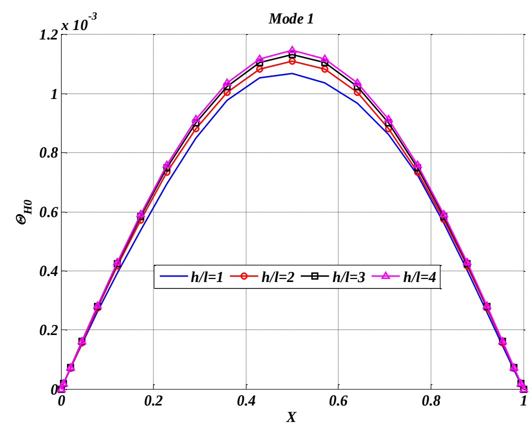

Fig. 9. The effect of material length scale parameter on the dimensionless magnetic potential (mode 1) for micro-beam (0)based on MSGT
$(\Delta T_0 = \Delta T_2 = \Omega_{H0} = \Omega_{H2} = V_{E0} = V_{E2} = 0)$.

Figure 10 represent the effect of material length scale parameter on the dimensionless electric potential for micro-beam (0) based on MSGT (mode shapes 1). It is depicts from Figured 9 and 10 that the dimensionless magnetic potential and the dimensionless electric potential for micro-beam (0) increases with an increase in the aspect ratio. It is because that with increasing aspect ratio the thickness of micro – beam (0) increases and also the effect of magnetic and electric potential become more.

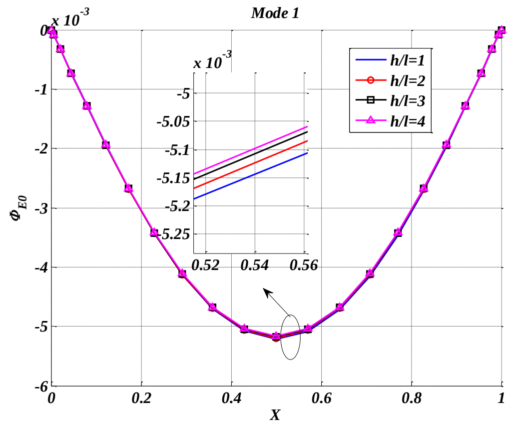

Fig. 10. The effect of material length scale parameter on the dimensionless electric potential (mode 1) for micro-beam (0)based on MSGT $(\Delta T_0 = \Delta T_2 = \Omega_{H0} = \Omega_{H2} = V_{E0} = V_{E2} = 0)$.

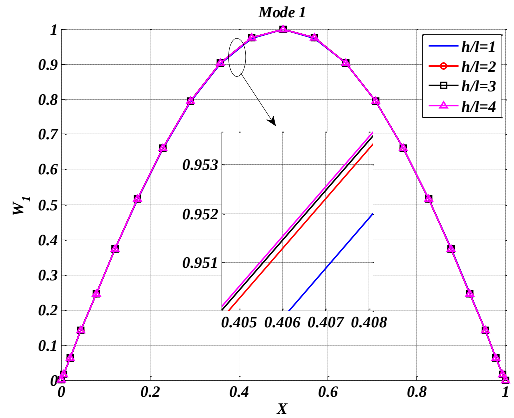

Fig. 12. The effect of material length scale parameter on the dimensionless deflection (mode 1) for micro-beam (1)based on MSGT $(\Delta T_0 = \Delta T_2 = \Omega_{H0} = \Omega_{H2} = V_{E0} = V_{E2} = 0)$.

Figure 11 present the rotation angle versus length of micro – beam (1) for different value of length scale parameters based on MSGT and mode shapes 1.

It is seen that from Figure 11 the value of rotation angle increases with increasing the aspect ratio. This means that micro-beam exhibits flexibly due to increasing aspect ratio.

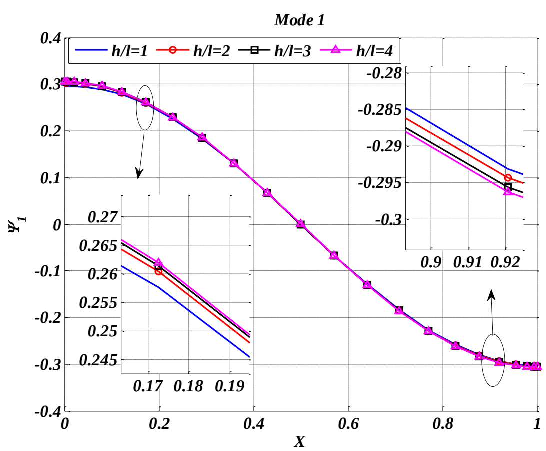

Fig. 11. rotation angle (mode 1) versus length of micro-beam (1) for various material length scale parameters based on MSGT $(\Delta T_0 = \Delta T_2 = \Omega_{H0} = \Omega_{H2} = V_{E0} = V_{E2} = 0)$.

Figure 12 show the effect of material length scale parameter on the dimensionless transverse deflection (mode shapes 1) for micro-beam (1) based on MSGT. Figure 12 depicts that the value of dimensionless transverse displacement increasing with an increases the value of aspect ratio.

These observations mean that with increasing aspect ratio the micro-beam become more flexible.

CONCLUSION

In this article, the free vibration analysis of smart micro-beam based on Reddy – Levinson model and modified strain gradient theory is developed. This system concluded a micro beam at middle and two magneto-electro-elastic composite micro beams at top and bottom which connected by enclosing elastic medium and simulated by Winkler and Pasternak foundation.

MEE micro beams are subjected to the external electric voltage, magnetic potential and temperature change.

Governing equations of motion and boundary conditions are derived using Hamilton's principle. The differential quadrature method is employed to solve them. The effects of external magnetic potential, electric voltage, temperature change, elastic foundation, dimensionless magnetic and electric potentials, material length scale parameter and slenderness ratio on the dimensionless natural frequency are investigated.

The results of this research can be stated as:

1- It is found that by increasing the external electric voltage and temperature change, the dimensionless natural frequency of system decreases whereas this is contrary to the external magnetic potential.

2- By increasing the value of aspect ratio, dimensionless natural frequencies at (RLBM) and (TBM) for MSGT and MCST decreases and for CT is constant.

3- Dimensionless natural frequencies at (RLBM) is higher than (TBM) for each three MSGT, MCST and CT and each aspect ratio.

4- The smart micro – beam system have less dimensionless natural frequencies than micro-beam (1) system only and MEE composite micro – beam (0) with micro-beam (1) together.

5- It is shown that by increasing the external magnetic potential on the MEE micro beams, the dimensionless natural frequency of the smart micro- beam system increases. Also, it can be observed that the influence of the external electric voltage on the dimensionless natural frequency for smart micro- beam system in higher slenderness ratio is more.

Furthermore, the dimensionless natural frequency of the smart micro- beam system decreases with increasing of the external electric voltage on the MEE micro beams.

6- It is concluded that with an increase in the temperature change of MEE microbeam (0), dimensionless natural frequency of smart micro- beam system decreases.

7-The effect of material length scale parameter on the dimensionless electric potential for micro-beam (0) based on MSGT (mode shapes 1) is investigated. The dimensionless natural frequencies at each three system for MSGT are higher than for MCST and CT. Because of considering three material length scale parameters leads to enhance more stiffness of micro structures.

REFERENCES

[1] Nilsson SG, Sarwe .L, Montelius L. Fabrication and mechanical characterization of ultrashort nano cantilevers. J. 2003;83:990-993.

[2] Rahaeifard M, Kahrobaiyan MH, Ahmadian MT. Sensitivity analysis of atomic force microscope cantilever made of functionally graded materials. ASME. Int. Des. Tech. Conf. and Comput. and Inf. Eng. Conf. 2009.

[3] Nilsson SG, Borrise X, Montelius L. Size Effect on Young's Modulus of Thin Chromium Cantilevers. J. Appl. Phys. 2004;85:3555-3557.

[4] Li X, Bhushan B, Baek C.W, Kim YK. Mechanical characterization of micro/nanoscale structures for MEMS/NEMS applications using nano indentation techniques. 2003;97:481–494.

[5] Zhai J, Xing Z, Dong S. Li J, Viehland D. Magnetoelectric laminate composites: an overview, J. Am. Ceram. Soc. 2008;91: 351–358.

[6] Van den Boomgaard J, Terrell D, Born R, Giller H. An in situ grown eutectic magnetoelectric composite material. J. Mater. Sci. 1974;9:1705-1709.

[7] Xu XJ, Deng ZC, Zhang Z, Meng JM. Surface effects on the bending, buckling and free vibration analysis of magneto-electro-elastic beams. Acta. Mech 2016; DOI: 10.1007/s00707-016-1568-7.

[8] Li J, Dunn M. Micromechanics of magneto-electro-elastic composite materials: average fields and effective behavior. J. Intell. Mater. Syst. Struct. 2015;119:377–384.

[9] Razavi S, Shooshtari A. Nonlinear free vibration of magneto-electro-elastic rectangular plates. Compos. Struct. 2015;119: 377–384.

[10] Ghorbanpour Arani A, Abdollahian M, Kolahchi R, Nonlinear vibration of a nanobeam elastically bonded with a piezoelectric nanobeam via strain gradient theory. Int. J. Mech. Sci. 2015;10032-40.

[11] Pisarskia D, Bajera CI, Dyniewicza B, Bajkowskib JM. Vibration control in smart coupled beams subjected to pulse excitations. J. Sound. Vib. 2016 ;380:37-50.

[12] Ebrahimi F, barati MR. Magnetic field effects on buckling behavior of smart size-dependent graded nanoscale beams. Eur. Phys. J. Plus. 131:238. DOI 10.1140/epjp/i2016-16238-8.

[13] Vaezi M, MooriShirbani M, Hajnayeb A. Free vibration analysis of magneto-electro-elasticmicrobeams subjected to magneto-electric Loads. Phys. E. DOI:http//dx doj org/10 1016/j phvse 09019.

[14] Farajpour A, HairiYazdi MR, Rastgoo A, Loghmani A, Mohammadi M. Nonlocal nonlinear plate model for large amplitude vibration of magneto-electro-elastic nanoplates. Compos. Struct. 2016;140: 323–336.

[15] Kattimani S.C, Ray MC. Control of geometrically nonlinear vibrations of functionally graded magneto-electroelastic plates. 2015;19: 154–167.

[16] Gharib A, Karimi MS, Ghorbanpour Arani A. Vibration analysis of the embedded piezoelectric polymeric nano-composite panels in the elastic substrate. Compos. part.B.

[17] Ghorbanpour Arani A, Jamali M, Mosayyebi M, Kolahchi R. Wave propagation in FG-CNT-reinforced piezoelectric composite micro plates using viscoelastic quasi-3D sinusoidal shear deformation theory. Compos. Part. B. DOI: 10.1016/j.compositesb 03.077.

[18] Wang W, Li P, Jin F, Wang J. ibration analysis of piezoelectric ceramic circular nanoplates considering surface and nonlocal effects. Compos. Struct. DOI: http://dx.doi.org/10.1016/j.compstruct.01.035.

[19] Chen JY, Heyliger PR, Pan E. Free vibration of three-dimensional multilayered magneto-electro-elastic plates under combined clamped/free boundary conditions. J. Sound. Vib. 2014;333: 4017–4029.

[20] Arefi M. Analysis of wave in a functionally graded magneto-electroelastic nano-rod using nonlocal elasticity model subjected to electric and magnetic potentials. Acta. Mech. DOI: 10.1007/s00707-016-1584-7.

[21] Shooshtari A, Razavi S. Linear and nonlinear free vibration of a multilayered magneto-electro-elastic doubly-curved shell on elastic foundation. Compos. Part. B. 2015;78: 95-108.

[22] Shooshtari A, Razavi S. Large amplitude free vibration of symmetrically laminated magneto-electro-elastic rectangular plates on Pasternak type foundation. Compos. Struct. 2015;119: 377–384.

[23] Li YS, Feng WJ. Microstructure-dependent piezoelectric beam based on modified strain gradient theory. Smart. Mater. Struct. 2014;23: 095004.

[24] Ke LL, Wang YS. Free vibration of size-dependent magneto-electro-elastic nanobeams based on the nonlocal theory. Phys. E. 2014;63: 52-61.

[25] Ansari R, Gholami R, Rouhi H. Size-dependent nonlinear forced vibration analysis of magneto-electro-thermoelastic Timoshenko nanobeams based upon the nonlocal elasticity theory. Compos. Struct. 2015;126: 216–226.

[26] Ansari R, Hasrati E, Gholami R, Sadeghi F. Nonlinear analysis of forced vibration of nonlocal third-order shear deformable beam model of magneto – electro - thermo elastic nanobeams. Compos. Part. B. 2015;83: 226-241.

[27] Atabakhshian V, Shooshtari A, Karimi M. Electro-thermal vibration of a smart coupled nanobeam system with an internal flow based on nonlocal elasticity theory. Phys. B. 2015;456: 375–382.

[28] Mohammadimehr M, RoustaNavi B, GhorbanpourArani A. Modified strain gradient Reddy rectangular plate model for biaxial buckling and bending analysis of double-coupled piezoelectric polymeric nanocomposite reinforced by FG-SWNT, Compos. Part. B: Eng. 2016;87: 132-148.

[29] Mohammadimehr M, RoustaNavi B, GhorbanpourArani A. Free vibration of viscoelastic double-bonded polymeric nanocomposite plates reinforced by FG-SWCNTs using MSGT, sinusoidal shear deformation theory and meshless method. Compos. Struct. 2015;131: 654-671.

[30] Reddy JN. A simple higher-order theory for laminated composite plates. J. Appl. Mech. 1984;5:745–752.

[31] Levinson M. A new rectangular beam theory. J. Sound. Vib. 1981;74: 81–87.

[32] Reddy J. A refined nonlinear theory of plates with transverse shear deformation. Int. J. Solids. and Struct. 1984: 20881-20896

[33] Lam DDC, Yang F, Chong ACM, Wang J, Tong P. Experiments and theory in strain gradient elasticity. J. Mech. Phys. Solids. 2003;51:1477–15083.

[34] Yang F, Chong ACM, Lam DDC. Couple stress based strain gradient theory for elasticity. Int. J. Solids. Struct. 2002;39:2731–43.

[35] Mohammadimehr M, Mostafavifar M. Free vibration analysis of sandwich plate with a transversely flexible core and FG-CNTs reinforced nanocomposite face sheets subjected to magnetic field and temperature-dependent material properties using SGT. Compos. part. B. DOI: 10.1016/j.compositesb.03.030.

[36] Zhang B, He Y, Liu D, Gan ZH, L. Shen L. Size-dependent functionally graded beam model based on an improved third-order shear deformation theory. Europ. J. Mech. A/Solids. 2014;47:211-230.

[37] Li YS, Feng WJ, Cai ZY. Bending and free vibration of functionally graded piezoelectric beam based on modified strain gradient theory. Compos. Struct. 2014;115:41-50.

[38] Sun KH, Kim YY. Layout design optimization for magneto-electro-elastic laminate composites for maximized energy conversion under mechanical loading. Smart. Mater. Struct. 2010;19:055008.

[39] Kahrobaiyan MH, Asghari M, Ahmadian MT. A strain gradient Timoshenko beam element: application to MEMS. Acta. Mech. 2015;226:505–525.

[40] Liua J, Zhanga P, Lina G, Wanga W, Lua SH. High order solutions for the magneto-electro-elastic plate with non-uniform materials. Int. J. Mech. Sci. DOI: http://dx.doi.org/10.1016/j.ijmecsci.07.033.

[41] TadiBeni Y, Karimipour I, Abadyan M. Modeling the instability of electrostatic nano-bridges and nano-cantilevers using modified strain gradient theory. Appl. Math. Model. 2015;39:2633–2648.

[42] Karimipour I, Tadi Beni Y, Koochi, Abadyan M. Using couple stress theory for modeling the size-dependent instability of double-sided beam-type nanoactuators in the presence of Casimir force. J. Braz. Soc. Mech. Sci. Eng. DOI 10.1007/s40430-015-0385-6.

[43] Komijani M, Reddy JN, Eslami MR. Nonlinear analysis of microstructure-dependent functionally graded piezoelectric material actuators. J. Mech. Phys. Solids. 2014;63:214–27.

[44] Sahmani S, Bahrami M. Size-dependent dynamic stability analysis of microbeams actuated by piezoelectric voltage based on strain gradient elasticity theory. J. Mech. Sci. Technol. 2015;29:325-333.

[45] Khodami Maraghi Z, GhorbanpourArani A, Kolahchi R, Amir S, Bagheri MR. Nonlocal vibration and instability of embedded DWBNNT conveying viscose fluid. Compos. Part. B. 2013;45: 423–432.

[46] Hatami M, Ganji DD. Motion of a spherical particle in a fluid forced vortex by DQM and DTM. Particuology. 2014;16:206–212.

[47] Akbari R, Alashti A, Ahmad SA. Buckling Analysis of Functionally Graded Thick Cylindrical Shells with Variable Thickness Using DQM. Arab. J. Sci. Eng. 2014;39:8121–8133.

[48] Alinaghizadeh F, Shariati M. Static analysis of variable thickness two-directional functionally graded annular sector plates fully or partially resting on elastic foundations by the GDQ method. J. Braz. Soc. Mech. Sci. Eng. DOI 10.1007/s40430-015-0427-0.

[49] Eftekhari SA. A simple and accurate mixed Ritz-DQM formulation for free vibration of rectangular plates involving free corners. Ain. Shams. Eng. J. 2016;7:777–790.

[50] Ghadiri M, Shafiei N. Vibration analysis of rotating functionally graded Timoshenko microbeam based on modified couple stress theory under different temperature distributions. Acta. Astron. 2016;121:221–240.

[51] Shafiei N, Kazemi M, Ghadiri M. Nonlinear vibration behavior of a rotating nanobeam underthermal stress using Eringen's nonlocal elasticity and DQM. Appl. Phys. A. DOI: 10.1007/s00339-016-0245-y.

[52] Lam DCC, Yang F, Chong ACM, Wang J, Tong P. Experiments and theory in strain gradient elasticity. J. Mech. Phys. Solids. 2003;51:1477–1508.
[53] Wang B, Liu M, Zhao J, Zhou SH. A size-dependent Reddy–Levinson beam model based on a strain gradient elasticity theory. Meccanica. 2014;49:1427–1441.

Appendix:

$$\begin{gathered}
\bar{c}_{11}=c_{11}-\frac{c_{13}^{2}}{c_{33}},\bar{c}_{44}=c_{44},\bar{e}_{31}=e_{31}-\frac{c_{13}e_{33}}{c_{33}},\bar{e}_{15}=e_{15}\\
,\bar{q}_{31}=q_{31}-\frac{c_{13}q_{33}}{c_{33}}\\
\bar{s}_{11}=s_{11},\bar{s}_{33}=s_{33}+\frac{e_{33}^{2}}{c_{33}},\bar{d}_{11}=d_{11},\bar{d}_{33}=d_{33}+\frac{e_{33}q_{33}}{c_{33}}\\
,\bar{\alpha}_{11}=\alpha_{11},\bar{\alpha}_{33}=\alpha_{33}+\frac{q_{33}^{2}}{c_{33}}\\
\bar{q}_{15}=q_{15},\bar{\beta}_{1}=\beta_{1}-\frac{c_{13}\beta_{3}}{c_{33}},\bar{\nu}_{3}=\nu_{3}+\frac{e_{33}\beta_{3}}{c_{33}},\bar{\lambda}_{3}=\lambda_{3}+\frac{q_{33}\beta_{3}}{c_{33}}
\end{gathered}\tag{A-1}$$

$$\begin{gathered}
\begin{Bmatrix}\mathrm{M},\mathrm{M}^{*}\\R,R^{*}\end{Bmatrix}=\int_{A}\begin{Bmatrix}z\\z^{3}\end{Bmatrix}\left\{\sigma_{xx},\sigma_{xx}^{*}\right\}dA\\
,\begin{Bmatrix}Q,Q^{*}\\F,F^{*}\end{Bmatrix}=\int_{A}\begin{Bmatrix}1\\z^{2}\end{Bmatrix}\left\{\sigma_{xz},\sigma_{xz}^{*}\right\}dA\\
\begin{Bmatrix}P_{1}^{(1)},P_{1}^{*(1)}\\P_{1}^{(3)},P_{1}^{*(3)}\end{Bmatrix}=\int_{A}\begin{Bmatrix}z\\z^{3}\end{Bmatrix}\left\{P_{x},P_{x}^{*}\right\}dA\\
,\begin{Bmatrix}P_{3}^{(0)},P_{3}^{*(0)}\\P_{3}^{(2)},P_{3}^{*(2)}\end{Bmatrix}=\int_{A}\begin{Bmatrix}1\\z^{2}\end{Bmatrix}\left\{P_{z},P_{z}^{*}\right\}dA\\
,\begin{Bmatrix}Y_{12}^{(0)},Y_{12}^{*(0)}\\Y_{12}^{(2)},Y_{12}^{*(2)}\end{Bmatrix}=\int_{A}\begin{Bmatrix}1\\z^{2}\end{Bmatrix}\left\{m_{xy},m_{xy}^{*}\right\}dA\\
,\left\{Y_{32}^{(1)},Y_{32}^{*(1)}\right\}=\int_{A}z\left\{m_{yz},m_{yz}^{*}\right\}dA\\
\begin{Bmatrix}T_{111}^{(1)},T_{111}^{*(1)}\\T_{133}^{(1)},T_{133}^{*(1)}\\T_{122}^{(1)},T_{122}^{*(1)}\end{Bmatrix}=\int_{A}z\begin{Bmatrix}\tau_{111}^{(1)},\tau_{111}^{*(1)}\\\tau_{133}^{(1)},\tau_{133}^{*(1)}\\\tau_{122}^{(1)},\tau_{122}^{*(1)}\end{Bmatrix}dA\\
,\begin{Bmatrix}T_{333}^{(1)},T_{333}^{*(1)}\\T_{113}^{(0)},T_{113}^{*(0)}\\T_{322}^{(0)},T_{322}^{*(0)}\end{Bmatrix}=\int_{A}\begin{Bmatrix}\tau_{333}^{(1)},\tau_{333}^{*(1)}\\\tau_{113}^{(1)},\tau_{113}^{*(1)}\\\tau_{322}^{(1)},\tau_{322}^{*(1)}\end{Bmatrix}dA\\
\begin{Bmatrix}T_{333}^{(2)},T_{333}^{*(2)}\\T_{113}^{(2)},T_{113}^{*(2)}\\T_{322}^{(2)},T_{322}^{*(2)}\end{Bmatrix}=\int_{A}z^{2}\begin{Bmatrix}\tau_{333}^{(1)},\tau_{333}^{*(1)}\\\tau_{113}^{(1)},\tau_{113}^{*(1)}\\\tau_{322}^{(1)},\tau_{322}^{*(1)}\end{Bmatrix}dA\\
,\begin{Bmatrix}T_{111}^{(1)},T_{111}^{*(1)}\\T_{133}^{(1)},T_{133}^{*(1)}\\T_{122}^{(1)},T_{122}^{*(1)}\end{Bmatrix}=\int_{A}z^{3}\begin{Bmatrix}\tau_{111}^{(1)},\tau_{111}^{*(1)}\\\tau_{133}^{(1)},\tau_{133}^{*(1)}\\\tau_{122}^{(1)},\tau_{122}^{*(1)}\end{Bmatrix}dA
\end{gathered}\tag{A-2}$$

$$\begin{gathered}
X=\frac{x}{L},W_{i}=\frac{w_{i}}{h},\varphi_{i}=\Psi_{i},\Phi_{Ej}=\frac{\phi_{Ej}}{\phi_{j}},\Theta_{Hj}=\frac{\Upsilon_{Hj}}{\Upsilon_{j}},\phi_{j}=\sqrt{\frac{A_{44}}{X_{33}}},\Upsilon_{j}=\sqrt{\frac{A_{44}}{T_{33}}}\\
\tau=\frac{t}{L}\sqrt{\frac{A_{44}}{m_{0}}},(\mathrm{E}_{15},\mathrm{E}_{31},F_{15},F_{31})=(\frac{E_{15}^{(0)}\phi_{j}}{A_{44}h},\frac{E_{31}^{(1)}\phi_{j}}{A_{44}h},\frac{E_{15}^{(2)}\phi_{j}}{A_{44}h^{3}},\frac{E_{31}^{(3)}\phi_{j}}{A_{44}h^{3}})\\
(Q_{15},\mathrm{Q}_{31},G_{15},G_{31})=(\frac{Q_{15}^{(0)}\Upsilon_{j}}{A_{44}h},\frac{\mathrm{Q}_{31}^{(1)}\Upsilon_{j}}{A_{44}h},\frac{Q_{15}^{(2)}\Upsilon_{j}}{A_{44}h^{3}},\frac{Q_{31}^{(3)}\Upsilon_{j}}{A_{44}h^{3}})\\
(\hat{\mathrm{X}}_{11},\hat{X}_{33})=(\frac{X_{11}\varphi_{j}^{2}}{A_{44}h^{2}},\frac{X_{33}\varphi_{j}^{2}}{A_{44}}),(\hat{T}_{11},\hat{\mathrm{T}}_{33})=(\frac{T_{11}\Upsilon_{j}^{2}}{A_{44}h^{2}},\frac{T_{33}\Upsilon_{j}^{2}}{A_{44}}),\\
(\hat{\mathrm{Y}}_{11},\hat{\mathrm{Y}}_{33})=(\frac{Y_{11}\Upsilon_{j}\varphi_{j}}{A_{44}h^{2}},\frac{Y_{33}\Upsilon_{j}\varphi_{j}}{A_{44}})\\
,i_{66}=\frac{I_{66}L^{2}}{A_{44}},\hat{c}_{1}=c_{1}h^{2},(\ell_{0},\ell_{1},\ell_{2})=\frac{(\mathrm{l}_{0},\mathrm{l}_{1},\mathrm{l}_{2})}{h},\eta=\frac{L}{h}\\
,(\bar{N}_{mj},\bar{N}_{ej},\bar{N}_{tj})_{(j=0,2)}=(\frac{N_{mj},N_{ej},N_{tj}}{A_{44}}),(\mathrm{k}_{wn},\mathrm{k}_{gn})_{(n=a,b)}=(\frac{K_{wn}L^{2}}{A_{44}},\frac{K_{gn}}{A_{44}})\\
\begin{cases}(j_{33},k_{22},i_{22},k_{33},i_{33},j_{22})=\dfrac{(J_{33},K_{22},I_{22},K_{33},I_{33},J_{22})}{A_{44}h^{2}}\\(I_{100},I_{122},I_{144},I_{166})=(\dfrac{m_{0}}{m_{0}},\dfrac{m_{2}}{m_{0}h^{2}},\dfrac{m_{4}}{m_{0}h^{4}},\dfrac{m_{6}}{m_{0}h^{4}})\qquad \textit{also for}\ *\\(a_{44},i_{44},i_{55},j_{44},j_{55},a_{55})=\dfrac{(A_{44},I_{44},I_{55},J_{44},J_{55},A_{55})}{A_{44}}\end{cases}
\end{gathered}\tag{A-3}$$

where:

$$\begin{gathered}
\begin{Bmatrix}\mathrm{E}_{15}^{(0)}\\\mathrm{E}_{15}^{(2)}\end{Bmatrix}=\int_{A}\bar{e}_{15}\cos(\beta z)\begin{Bmatrix}1\\z^{2}\end{Bmatrix}\mathrm{dA},\begin{Bmatrix}Q_{15}^{(0)}\\Q_{15}^{(2)}\end{Bmatrix}=\int_{A}\bar{q}_{15}\cos(\beta z)\begin{Bmatrix}1\\z^{2}\end{Bmatrix}\mathrm{dA}\\
\begin{Bmatrix}\mathrm{E}_{31}^{(1)}\\\mathrm{E}_{31}^{(3)}\end{Bmatrix}=\int_{A}\bar{e}_{31}\beta\sin(\beta z)\begin{Bmatrix}z\\z^{3}\end{Bmatrix}\mathrm{dA},\begin{Bmatrix}Q_{31}^{(1)}\\Q_{31}^{(3)}\end{Bmatrix}=\int_{A}\bar{q}_{31}\beta\sin(\beta z)\begin{Bmatrix}z\\z^{3}\end{Bmatrix}\mathrm{dA}\\
\left\{\mathrm{X}_{11},Y_{11},T_{11}\right\}=\int_{A}\left\{\bar{s}_{11},\bar{d}_{11},\bar{\mu}_{11}\right\}\cos^{2}(\beta\mathrm{z})\mathrm{dA},\\
\left\{\mathrm{X}_{33},Y_{33},T_{33}\right\}=\int_{A}\left\{\bar{s}_{33},\bar{d}_{33},\bar{\mu}_{33}\right\}[\beta\sin(\beta z)z]^{2}\,\mathrm{dA}\\
\begin{cases}\bar{c}_{44}A=A_{44}\\\mu A=A_{55},c_{1}\mu I=I_{44},c_{1}\bar{c}_{11}J=J_{22}\\Ic_{1}\bar{c}_{44}=I_{55},I\mu=I_{33},c_{1}\mu J=J_{33}\\I\mu c_{1}^{2}=I_{66},I\bar{c}_{11}=I_{22},J\mu c_{1}^{2}=J_{44}\qquad \textit{also for}\ *\\K\mu c_{1}^{2}=K_{22},c_{1}^{2}\bar{c}_{11}K=K_{33},c_{1}^{2}\bar{c}_{44}J=J_{55}\\A=bh,I=\dfrac{bh^{3}}{12},J=\dfrac{bh^{5}}{80},K=\dfrac{bh^{7}}{448}\end{cases}
\end{gathered}\tag{A-4}$$

$$
\begin{aligned}
&\{(a_{44}-6i_{55}+9j_{55})+(\frac{96}{5}\ell_1^2+9\ell_2^2)\frac{i_{66}}{\eta^2}\}(\Psi_0-\frac{1}{\eta}\sum_1^N A_{ij}^{(1)}W_0)\\
&+\{-(i_{22}-2j_{22}+k_{33})-(2\ell_0^2+\frac{32}{15}\ell_1^2+\frac{1}{4}\ell_2^2)a_{55}\\
&+(12\ell_0^2+\frac{88}{5}\ell_1^2+\frac{3}{2}\ell_2^2)i_{44}-(18\ell_0^2+24\ell_1^2+\frac{9}{4}\ell_2^2)j_{44}\}(\frac{1}{\eta^2}\sum_1^N A_{ij}^{(2)}\Psi_0)\\
&+\{(k_{33}-j_{22})+(\frac{16}{15}\ell_1^2-\frac{1}{4}\ell_2^2)a_{55}-(6\ell_0^2+12\ell_1^2)i_{44}\\
&+(18\ell_0^2+24\ell_1^2+\frac{9}{4}\ell_2^2)j_{44}\}(\frac{1}{\eta^3}\sum_1^N A_{ij}^{(3)}W_0)\\
&+\{(2\ell_0^2+\frac{4}{5}\ell_1^2)(i_{33}+k_{22}-2j_{33})\}(\frac{1}{\eta^4}\sum_1^N A_{ij}^{(4)}\Psi_0)\\
&+\{E_{31}-F_{31}\hat{c}_1-3\hat{c}_1F_{15}+E_{15}\}(\frac{1}{\eta}\sum_1^N A_{ij}^{(1)}\Phi_{E0})\\
&+\{Q_{31}-\hat{c}_1G_{31}-3\hat{c}_1G_{15}+Q_{15}\}(\frac{1}{\eta}\sum_1^N A_{ij}^{(1)}\Theta_{H0})\\
&-\{(2\ell_0^2+\frac{4}{5}\ell_1^2)(k_{22}-j_{33})\}(\frac{1}{\eta^5}\sum_1^N A_{ij}^{(5)}W_0)\\
&+(\hat{c}_1^2I_{166}-2\hat{c}_1I_{144}+I_{122})(\frac{1}{\eta^2}\frac{\partial^2\Psi_0}{\partial\tau^2})\\
&+(\hat{c}_1I_{144}-\hat{c}_1^2I_{166})(\frac{1}{\eta^3}\frac{\partial^2}{\partial\tau^2}\sum_1^N A_{ij}^{(1)}W_0)=0
\end{aligned}
\qquad \text{(A-5)}
$$

$$
\begin{aligned}
&\{(a_{44}-6i_{55}+9j_{55})+(\frac{96}{5}\ell_1^2+9\ell_2^2)\frac{i_{66}}{\eta^2}\}(\sum_1^N A_{ij}^{(1)}\Psi_0\\
&-\frac{1}{\eta}\sum_1^N A_{ij}^{(2)}W_0)+\{(j_{22}-k_{33})+(-\frac{16}{15}\ell_1^2+\frac{1}{4}\ell_2^2)a_{55}\\
&+(6\ell_0^2+12\ell_1^2)i_{44}-(18\ell_0^2+24\ell_1^2+\frac{9}{4}\ell_2^2)j_{44}\}(\frac{1}{\eta^2}\sum_1^N A_{ij}^{(3)}\Psi_0)\\
&+(18\ell_0^2+24\ell_1^2+\frac{9}{4}\ell_2^2)j_{44}\}(\frac{1}{\eta^3}\sum_1^N A_{ij}^{(4)}W_0)\\
&+(\bar{N}_{m0}+\bar{N}_{e0}+\bar{N}_{t0})(\frac{1}{\eta})\sum_1^N A_{ij}^{(2)}W_0+(\frac{3}{2}\ell_2^2-\frac{32}{5}\ell_1^2)i_{44}\\
&+\{(2\ell_0^2+\frac{4}{5}\ell_1^2)(k_{22}-j_{33})\}(\frac{1}{\eta^4}\sum_1^N A_{ij}^{(5)}\Psi_0)\\
&-\{(2\ell_0^2+\frac{4}{5}\ell_1^2)(k_{22})\}(\frac{1}{\eta^5}\sum_1^N A_{ij}^{(6)}W_0)+\{k_{33}+(\frac{8}{15}\ell_1^2+\frac{1}{4}\ell_2^2)a_{55}\\
&+\{-\hat{c}_1F_{31}-3\hat{c}_1F_{15}+E_{15}\}(\frac{1}{\eta}\sum_1^N A_{ij}^{(2)}\Phi_{E0})\\
&+\{-\hat{c}_1G_{31}-3\hat{c}_1G_{15}+Q_{15}\}(\frac{1}{\eta}\sum_1^N A_{ij}^{(2)}\Theta_{H0})+\frac{k_{wa}}{\eta}(W_0-W_1)\\
&-\frac{K_{ga}}{\eta}\nabla^2(W_0-W_1)+(\hat{c}_1^2I_{166}-\hat{c}_1I_{144})(\frac{1}{\eta^2}\frac{\partial^2}{\partial\tau^2}\sum_1^N A_{ij}^{(1)}\Psi_0)\\
&-\frac{\hat{c}_1^2I_{166}}{\eta^3}\frac{\partial^2}{\partial\tau^2}(\sum_1^N A_{ij}^{(2)}W_0)+\frac{I_{100}}{\eta}\frac{\partial^2W_0}{\partial\tau^2}=0
\end{aligned}
\qquad \text{(A-6)}
$$

$$
\begin{aligned}
&-E_{31}\eta(\sum_1^N A_{ij}^{(1)}\Psi_0)-(3\hat{c}_1F_{15}+\hat{c}_1F_{31}-E_{15})(\sum_1^N A_{ij}^{(2)}W_0-\eta(\sum_1^N A_{ij}^{(1)}\Psi_0))\\
&+\hat{X}_{11}(\sum_1^N A_{ij}^{(2)}\Phi_{E0})+\hat{Y}_{11}(\sum_1^N A_{ij}^{(2)}\Theta_{H0})-\hat{X}_{33}\eta^2\Phi_{E0}-\hat{Y}_{33}\eta^2\Theta_{H0}=0
\end{aligned}
\qquad \text{(A-7)}
$$

$$
\begin{aligned}
&-Q_{31}\eta(\sum_1^N A_{ij}^{(1)}\Psi_0)-(3\hat{c}_1G_{15}+\hat{c}_1G_{31}-Q_{15})(\sum_1^N A_{ij}^{(2)}W_0-\eta(\sum_1^N A_{ij}^{(1)}\Psi_0))\\
&+\hat{Y}_{11}(\sum_1^N A_{ij}^{(2)}\Phi_{E0})+\hat{T}_{11}(\sum_1^N A_{ij}^{(2)}\Theta_{H0})-\hat{Y}_{33}\eta^2\Phi_{E0}-\hat{T}_{33}\eta^2\Theta_{H0}=0
\end{aligned}
\qquad \text{(A-8)}
$$

$$
\begin{aligned}
&\{(a_{44}^*-6i_{55}^*+9j_{55}^*)+(\frac{96}{5}\ell_1^{*2}+9\ell_2^{*2})\frac{i_{66}^*}{\eta^2}\}(\Psi_1-\frac{1}{\eta}\sum_1^N A_{ij}^{(1)}W_1)\\
&+\{-(i_{22}^*-2j_{22}^*+k_{33}^*)-(2\ell_0^{*2}+\frac{32}{15}\ell_1^{*2}+\frac{1}{4}\ell_2^{*2})a_{55}^*\\
&+(12\ell_0^{*2}+\frac{88}{5}\ell_1^{*2}+\frac{3}{2}\ell_2^{*2})i_{44}^*+\{(k_{33}^*-j_{22}^*)+(\frac{16}{15}\ell_1^{*2}-\frac{1}{4}\ell_2^{*2})a_{55}^*\\
&-(18\ell_0^{*2}+24\ell_1^{*2}+\frac{9}{4}\ell_2^{*2})j_{44}^*\}(\frac{1}{\eta^2}\sum_1^N A_{ij}^{(2)}\Psi_1)\\
&+(18\ell_0^{*2}+24\ell_1^{*2}+\frac{9}{4}\ell_2^{*2})j_{44}^*\}(\frac{1}{\eta^3}\sum_1^N A_{ij}^{(3)}W_1)-(6\ell_0^{*2}+12\ell_1^{*2})i_{44}^*\\
&-\{(2\ell_0^{*2}+\frac{4}{5}\ell_1^{*2})(k_{22}^*-j_{33}^*)\}(\frac{1}{\eta^5}\sum_1^N A_{ij}^{(5)}W_1)\\
&+\{(2\ell_0^{*2}+\frac{4}{5}\ell_1^{*2})(i_{33}^*+k_{22}^*-2j_{33}^*)\}(\frac{1}{\eta^4}\sum_1^N A_{ij}^{(4)}\Psi_1)\\
&+(\hat{c}_1^2I_{166}^*-2\hat{c}_1I_{144}^*+I_{122}^*)(\frac{1}{\eta^2}\frac{\partial^2\Psi_1}{\partial\tau^2})\\
&+(\hat{c}_1I_{144}^*-\hat{c}_1^2I_{166}^*)(\frac{1}{\eta^3}\frac{\partial^2}{\partial\tau^2}\sum_1^N A_{ij}^{(1)}W_1)=0
\end{aligned}
\qquad \text{(A-9)}
$$

$$
\begin{aligned}
&\{(a_{44}^*-6i_{55}^*+9j_{55}^*)+(\frac{96}{5}\ell_1^{*2}+9\ell_2^{*2})\frac{i_{66}^*}{\eta^2}\}(\sum_1^N A_{ij}^{(1)}\Psi_1\\
&-\frac{1}{\eta}\sum_1^N A_{ij}^{(2)}W_1)+\{(j_{22}^*-k_{33}^*)+(-\frac{16}{15}\ell_1^{*2}+\frac{1}{4}\ell_2^{*2})a_{55}^*\\
&-(18\ell_0^{*2}+24\ell_1^{*2}+\frac{9}{4}\ell_2^{*2})j_{44}^*\}(\frac{1}{\eta^2}\sum_1^N A_{ij}^{(3)}\Psi_1)\\
&+\{k_{33}^*+(\frac{8}{15}\ell_1^{*2}+\frac{1}{4}\ell_2^{*2})a_{55}^*+(\frac{3}{2}\ell_2^{*2}-\frac{32}{5}\ell_1^{*2})i_{44}^*\\
&+(18\ell_0^{*2}+24\ell_1^{*2}+\frac{9}{4}\ell_2^{*2})j_{44}^*\}(\frac{1}{\eta^3}\sum_1^N A_{ij}^{(4)}W_1)\\
&+\{(2\ell_0^{*2}+\frac{4}{5}\ell_1^{*2})(k_{22}^*-j_{33}^*)\}(\frac{1}{\eta^4}\sum_1^N A_{ij}^{(5)}\Psi_1)\\
&-\{(2\ell_0^{*2}+\frac{4}{5}\ell_1^{*2})(k_{22}^*)\}(\frac{1}{\eta^5}\sum_1^N A_{ij}^{(6)}W_0)+(6\ell_0^{*2}+12\ell_1^{*2})i_{44}^*\\
&-\frac{k_{wa}}{\eta}(W_0-W_1)+\frac{k_{ga}}{\eta}\nabla^2(W_0-W_1)\\
&+\frac{k_{wb}}{\eta}(W_1-W_2)-\frac{k_{gb}}{\eta}\nabla^2(W_1-W_2)\\
&+(\hat{c}_1^2I_{166}^*-\hat{c}_1I_{144}^*)(\frac{1}{\eta^2}\frac{\partial^2}{\partial\tau^2}\sum_1^N A_{ij}^{(1)}\Psi_1)\\
&-\frac{\hat{c}_1^2I_{166}^*}{\eta^3}\frac{\partial^2}{\partial\tau^2}(\sum_1^N A_{ij}^{(2)}W_1)+\frac{I_{100}^*}{\eta}\frac{\partial^2W_0}{\partial\tau^2}=0
\end{aligned}
\qquad \text{(A-10)}
$$

$$\begin{aligned}
&\{(a_{44}-6i_{55}+9j_{55})+(\frac{96}{5}\ell_1^2+9\ell_2^2)\frac{i_{66}}{\eta^2}\}(\sum_1^N A_{ij}^{(1)}\Psi_2\\
&-\frac{1}{\eta}\sum_1^N A_{ij}^{(2)}W_2)+\{(j_{22}-k_{33})+(-\frac{16}{15}\ell_1^2+\frac{1}{4}\ell_2^2)a_{55}\\
&+(6\ell_0^2+12\ell_1^2)i_{44}-(18\ell_0^2+24\ell_1^2+\frac{9}{4}\ell_2^2)j_{44}\}(\frac{1}{\eta^2}\sum_1^N A_{ij}^{(3)}\Psi_2)\\
&+\{k_{33}+(\frac{8}{15}\ell_1^2+\frac{1}{4}\ell_2^2)a_{55}+(\frac{3}{2}\ell_2^2-\frac{32}{5}\ell_1^2)i_{44}\\
&+(18\ell_0^2+24\ell_1^2+\frac{9}{4}\ell_2^2)j_{44}\}(\frac{1}{\eta^3}\sum_1^N A_{ij}^{(4)}W_2)\\
&+(\bar{N}_{m2}+\bar{N}_{e2}+\bar{N}_{t2})(\frac{1}{\eta})\sum_1^N A_{ij}^{(2)}W_2\\
&+\{(2\ell_0^2+\frac{4}{5}\ell_1^2)(k_{22}-j_{33})\}(\frac{1}{\eta^4}\sum_1^N A_{ij}^{(5)}\Psi_2)\\
&-\{(2\ell_0^2+\frac{4}{5}\ell_1^2)(k_{22})\}(\frac{1}{\eta^5}\sum_1^N A_{ij}^{(6)}W_2)\\
&+\{-\hat{c}_1F_{31}-3\hat{c}_1F_{15}+E_{15}\}(\frac{1}{\eta}\sum_1^N A_{ij}^{(2)}\Phi_{E2})\\
&+\{-\hat{c}_1G_{31}-3\hat{c}_1G_{15}+Q_{15}\}(\frac{1}{\eta}\sum_1^N A_{ij}^{(2)}\Theta_{H2})-\frac{k_{wb}}{\eta}(W_1-W_2)\\
&+(\hat{c}_1^2I_{166}-\hat{c}_1I_{144})(\frac{1}{\eta^2}\frac{\partial^2}{\partial\tau^2}\sum_1^N A_{ij}^{(1)}\Psi_2)+\frac{k_{gb}}{\eta}\nabla^2(W_1-W_2)\\
&-\frac{\hat{c}_1^2I_{166}}{\eta^3}\frac{\partial^2}{\partial\tau^2}(\sum_1^N A_{ij}^{(2)}W_2)+\frac{I_{100}}{\eta}\frac{\partial^2W_2}{\partial\tau^2}=0
\end{aligned}\tag{A-11}$$

$$\begin{aligned}
&-(3\hat{c}_1F_{15}+\hat{c}_1F_{31}-E_{15})(\sum_1^N A_{ij}^{(2)}W_2-\eta(\sum_1^N A_{ij}^{(1)}\Psi_2))\\
&+\hat{X}_{11}(\sum_1^N A_{ij}^{(2)}\Phi_{E2})+\hat{Y}_{11}(\sum_1^N A_{ij}^{(2)}\Theta_{H2})\\
&-E_{31}\eta(\sum_1^N A_{ij}^{(1)}\Psi_2)-\hat{X}_{33}\eta^2\Phi_{E2}-\hat{Y}_{33}\eta^2\Theta_{H2}=0
\end{aligned}\tag{A-12}$$

$$\begin{aligned}
&-(3\hat{c}_1G_{15}+\hat{c}_1G_{31}-Q_{15})(\sum_1^N A_{ij}^{(2)}W_2-\eta(\sum_1^N A_{ij}^{(1)}\Psi_2))\\
&+\hat{Y}_{11}(\sum_1^N A_{ij}^{(2)}\Phi_{E2})+\hat{T}_{11}(\sum_1^N A_{ij}^{(2)}\Theta_{H2})\\
&-Q_{31}\eta(\sum_1^N A_{ij}^{(1)}\Psi_2)-\hat{Y}_{33}\eta^2\Phi_{E2}-\hat{T}_{33}\eta^2\Theta_{H2}=0
\end{aligned}\tag{A-13}$$